Response to Reviewer Comments

We are thankful to the reviewers for their constructive and thoughtful comments that helped improving the manuscript. We have revised the manuscript according to these comments and added a supplement including further information on the AMS and PMF data quality assurance. Listed below is our point-by-point response to each of the reviewers' comments (red).

In addition, we received revised information on the time interval defined as "dust" period from the EC-LIFE+ DIAPASON project team: As a consequence of results from additional PIXE analysis they have changed the "dust" period for the DIAPASON2013 field campaign to 23.10.-01.11.2013 (before: 29.10.-01.11.2013) (Barnaba et al., in preparation 2016). This period includes days (23.-29.10.13) with rather low concentrations of coarse particles; however PIXE results and model calculations clearly indicate the presence of dust at ground level during these days. To avoid discrepancies and to allow for a better comparability between our results and those from their measurements, we therefore have adapted the period of the 2013 dust event in our manuscript and have revised our analysis in Sect. 4.2.1 accordingly. The no dust period is now defined as the period 02.11.-07.11.13 (before: 23.-28.10 + 02.11.-07.11.13). Extending the period of the dust event in 2013 did not cause any substantial changes in the conclusion. With respect to the background conditions, the PM_{10} fraction was increased (from 13 to 17 µg m^{-3}), whereas the coarse particle fraction ($PM_{10-2.5}$) was decreased (from 3.1 to 2.4 µg m^{-3}). While absolute concentrations of the AMS species have changed for the dust (increase of 5%) and no dust (decrease of 50%) period, the relative composition remains nearly the same. The strong decrease of the PM_1 fraction observed for the "new" no dust period likely results from a change in air mass origin. In the "old" definition the no dust period was composed of two time intervals, one before and one after the dust event, whereas in the "new" definition the no dust period only includes the period after the dust event. In this "new" no dust period, a change of air masses (Mediterranean region to Atlantic Ocean) occurred. While the "old" no dust period was influenced by air masses both from the Mediterranean region and the Atlantic Ocean, the "new" no dust period is preferentially influenced by air masses from the Atlantic Ocean. Furthermore, during the no dust period higher wind speeds were observed compared to the dust period, resulting in stronger dilution effects. This is briefly discussed in the revised manuscript (P15, L19-22).

All changes that have been made to the manuscript can be tracked in the attached version. When referring to the manuscript, we always refer to the page and line number of the revised manuscript including the track changes.

Response to anonymous referee #1

We thank anonymous referee #1 for his/her helpful comments.

General comments:

Comment: The manuscript by Struckmeier et al. analyzed four datasets that were collected at two sites in different seasons in Rome (suburban vs. urban). This study contains various real-time online measurements including aerosol chemical composition, gaseous species, particle number concentrations, and meteorological parameters. The sources of organic aerosols (OA) were also analyzed with positive matrix factorization. While rich chemical information was provided in this work to address the sources, dynamics, and spatial variations, the discussions e.g., composition, dust event, new particle formation, OA, and CSOA are scattered and lack of focus.

Reply: The intention and focus of our manuscript is to provide an assessment of the sub-micron aerosol and its potential sources at an urban and a suburban location in the Rome area during different measurement periods. This includes a general overview (the "rich chemical information" mentioned by the reviewer), but also deeper discussion on specific areas, which need to be addressed in order to characterize a complex urban environment like Rome. In particular with respect to the very different sources it would have been incomplete if for example the Saharan dust or the NPF, or other aspects had been left out. Thus, the focus of our work is on the description and, if possible, explanation of aerosols from the various sources, similar to approaches in previous publications from different groups (e.g., Crippa et al., 2013b; Kostenidou et al., 2015) which show that there is a general interest in this kind of analysis.

Specific comments:

Comment: Also, I have several major concerns on data analysis and the interpretations: (1) each campaign lasted less than two weeks, and most importantly, the measurements at the suburban and urban sites were not simultaneous. This clearly increases the uncertainties in comparing aerosol chemistry and sources between the two sites. In addition, it is difficult to see the dynamic variations of aerosol species in Rome if the authors didn't present time series data.

Reply: The durations of the data acquisition periods are in detail:

DIAPASON2013: 16 days of measurements (including 14 full days)

POPE2013: 8 days of measurements (including 6 full days)

DIAPASON2014: 16 days of measurements (including 14 full days)

POPE2014: 14 days of measurements (including 12 full days)

This shows that only POPE2013 was shorter than two weeks. The measurements were performed subsequently and not simultaneously as stressed in the manuscript, e.g., in the first sentence of the abstract. Obviously this results in a larger uncertainty when comparing the observations from the urban and suburban site, as the reviewer correctly states. This is why we do not generalise observations or differences in observations at different locations or during different seasons, but rather present our findings considering potentially different weather conditions etc., as clearly indicated several times in the manuscript, e.g.:

- P12, L33-P13, L3: "Regarding absolute PM_1 concentrations […] neither any general conclusion whether aerosol mass concentrations are higher at the city centre or in the suburb, nor whether PM_1 concentrations are elevated during any of the two different seasons, can be drawn."
- P13, L5-7: "As discussed above, changes in meteorological conditions are likely one explanation for this result …"

- L13, L12-14: “In addition to meteorological conditions (e.g. solar radiation, BLH, TKE, air mass origin, etc.) local air quality can be strongly influenced by local emission from various sources (traffic, cooking, biomass burning).”

Nevertheless, each of the four measurement intervals provides valuable information on properties and dynamics of various aerosol types in the city centre and at the suburban location, which are found to be sufficiently robust within the available measurement time.

In our manuscript we focus on general features of the observed aerosols. Therefore we did not show time series of aerosol variables. In order to allow the reader to get a picture on temporal variations during the field measurements, we added a supplement presenting time series of all PMF factors and some selected important other aerosol variables.

Comment: (2) the data quality was not validated adequately, particularly the AMS measurements. A simple comparison between PM1 measured by EDM and that measured by AMS and MAAP (NR-PM1 + BC) will help.

Reply: We agree that assuring data quality is good practice. During the analysis of the AMS (and other instruments’) data all standard procedures, checks, calibrations, corrections, intercomparisons, etc. have been performed (see statements in Sections 3.1 and 3.2). Besides other necessary quality checks, also comparison of AMS plus BC data with independent PM_1 data (EDM, but also PM_1 calculated from size distribution measurements) was performed as well as many other comparisons. All comparisons showed reasonable agreement (e.g., for PM_1 from AMS+BC versus EDM, R^2=0.69-0.85, Slopes: 0.73-1.37). We included the time series and scatter plots of AMS+BC and EDM PM_1 in the supplement, as well as a short discussion of the intercomparisons.

Comment: (3) the AMS data analysis needed to be expanded. For example, which approach (Aiken et al., 2008 or Canagaratna et al., 2015) was used to calculate the elemental ratios the calculation of elemental ratios? If there are elemental ratios, why did the authors still use f43 and f44 to discuss the oxidation states?

Reply: The results from AMS measurements were inspected for relationships among these data and relationships with data from other instruments. For the data obtained with the AMS and the other instruments temporal evolution, diurnal patterns and individual events were analysed (see Section 4).

Elemental ratios were calculated based on the current state of the art method (Canagaratna et al., 2015). We thank the reviewer for pointing out this missing information, which we added to the revised manuscript (P7, L22-23).

Our discussion using f43 and f44 focused on the aerosol aging levels, for which the “triangle” introduced by Ng et al. (2010) is commonly used (e.g., Ortega et al., 2016; Xu et al., 2016; Zhang et al., 2015). We also calculated elemental ratios for the various factors, but didn’t include them in the discussion on aerosol aging levels since they show equivalent behaviour as the f44/f43 data. For more completeness, we added the elemental ratios of each PMF factor to the supplement.

Comment: (4) the PMF analysis is a big weakness of this study. The authors didn't have a full evaluation of the PMF results. At least, the authors need to present the mass spectral profiles and times series of all OA factors, and also the comparisons with collocated measurements.

Reply: The performed PMF analysis and corresponding tests are subject of Section 3.2. All typical and many other tests to validate the results were applied, amongst others those according to the guidelines by Zhang et al. (2011), Table 1. All relevant information (e.g. m/z-range used for PMF, method of error and data matrix preparation, treatment of isotopes, treatment of low S/N data, treatment of CO_2-related ions, range of factors, fPeak and seed investigated) is detailed in the text.

Furthermore, each PMF factor was inspected for reasonability and validated by comparing factor time series with external species and mass spectral profiles with such from literature. Details are given in the text, e.g., P8, L18-20; P20, L25-29; P21, L17-23; P23, L5-9; P24, L5-8; P25, L1 -P26, L4.

So far we did not present all individual correlation plots and mass spectra in graphs, but presented this information in the form of R^2 values to save journal space and keep the length of the manuscript at a reasonable level without losing information. For more completeness we now added the mass spectral profiles and the time series of all PMF factors, as well as the time series of collocated measurements of tracer species and their correlations with PMF factors to the supplement.

Comment: The diurnal correlations the authors mentioned in page 21 did not mean much.

Reply: Such correlations are commonly used to show potential relationships between variables (e.g., Sun et al., 2016; Zhang et al., 2014), and to validate PMF factors (Zhang et al., 2011). In P23 we discuss that the diurnal patterns of HOA correlate well with those of other typically traffic-related species (BC, NOx, PAH). As stated in P23, L8-9, not only the diurnal cycles, but also the time series correlate well. To allow the reader to check this also for the temporal variations in the original time series, the time series of HOA and BC were also added to the supplement.

Comment: Figure 2 also showed substantial differences in HOA/BC ratios at the two sites in different seasons, and surprising BC contributions, which should be well interpreted.

Reply: We thank the reviewer for this valuable comment, and added some more discussion on this topic. We agree that there are differences in the HOA/BC ratios observed during the fall 2013 campaigns and during the spring 2014 campaigns (fall 2013: 0.26-0.33; spring 2014: 0.46-0.53). We attribute this to the fact that both, biomass burning and traffic contribute to total BC, as mentioned on P10, L29-30. Biomass burning is more predominant in fall, leading to higher BC mass concentrations, and therefore lower HOA/BC ratios during this season. The fact that larger ratios were found in the city centre in both seasons reflects the lower contribution of biomass burning emissions at this site. The contribution of different sources (traffic and biomass burning) also explains why the ratio of HOA/BC from our study is different to such ratios found in source measurements of pure traffic-related emissions.

Separation of BC related to the two sources unfortunately is not possible with the instrument used (MAAP), but measurements in other cities with the aethalometer instrument (e.g., Crippa et al., 2013a) have shown that BC contributions from biomass burning to total BC can be non-negligible. In the revised manuscript we extended the discussion of the aerosol composition and added to Sect. 4.1 (P10, L31-P11, L4):

"Ratios of HOA/BC (DIAPASON2013: 0.26, POPE2013: 0.33, DIAPASON2014: 0.46, POPE2014: 0.53) were lower during fall 2013, indicating the more dominant contribution of biomass burning emissions to BC during this time. The fact that contributions from biomass burning to total BC concentrations are non-negligible was also found earlier (e.g. Crippa et al. (2013a). Generally, the HOA/BC ratios were higher in the urban compared to the suburban location in each year. This reflects the stronger influence of traffic emissions and the lower contribution of biomass burning emissions in the city centre."

Comment: The PMF uncertainties lead to another major concern of the cigarette smoking factor. Although the authors concluded this as a major finding and presented a long discussion on it, it is still not convincing due to the limited resolution of V-mode (C5H10N+) and the absence of the measurements of molecular markers for cigarette smoking. I am also suspicious that the diurnal profile of CSOA did not reflect cigarette smoking that is expected less affected by boundary layer dynamics (if the authors claimed it as a point source). Showing the times series of CSOA factor will help.

Reply: PMF analysis is always associated with uncertainties. As described in the manuscript we have taken all care in order to minimize these uncertainties and we have made multiple tests and comparisons with other data (e.g. mass spectra of previously identified CSOA, as described in the manuscript and now also shown in the added supplementary information) in order to obtain results as robust as possible. While the CSOA factor was first obtained from the PMF analysis of the whole mass spectra, afterwards the $C_5H_{10}N^+$ marker was identified and found to have time series that correlate very well with those of CSOA. Indeed, as discussed in the manuscript, CSOA has been identified before from AMS data in which the newly found marker fragment at m/z 84 was not fitted at all (Faber et al., 2013) and yielded a very similar factor mass spectrum with correlation coefficients $0.65<R^2<0.96$ (P25, L31). (Re-analysis later showed that the marker fragment indeed was present also in these data, as discussed in the manuscript, P26 L9-11.) Therefore, and from other tests we performed in the data evaluation and quality assurance of the PMF-results, the retrieval of CSOA seems robust to us.

We agree that V-mode has a limited resolution, and we would not generally use it for determination of N-containing ion fragments. In the particular instance of m/z 84, contributions of C,H,O-containing fragments are rather small, which makes it possible to distinguish the N-containing marker fragment with reasonable certainty even in V-mode. Figure S16 in the supplementary information shows a typical fit on m/z 84, based on a 30 s run. As can be seen, the N-containing fragment can be clearly distinguished.

Of course the separation and fitting of $C_5H_{10}N^+$ only works as long as CSOA contributes sufficiently to the total m/z 84 signal with respect to contributions from POA_{noCSOA} (primary organic aerosol excluding cigarette smoke), as we discuss in the manuscript (P27,L7-17). We also discussed the limitations of identification and quantification of CSOA using this marker, taking into account the limited resolution of the V-mode (P27, L26-P28, L6).

Concerning “the absence of the measurements of molecular markers for cigarette smoking” we identified the fragment ion $C_5H_{10}N^+$ as an indication of nicotine, which is a molecular marker. While we do not have independent measurements of the same marker using different methods, we used the very good correlation of the time series of this marker ion and the CSOA factor to associate this marker ion with cigarette smoke. The fact that the marker ion was also found in laboratory measurements of cigarette smoke (see discussion on P26, L6-11) gives us confidence in its applicability.

Concerning the referee’s comment on the time series / diurnal profile: If the time series are affected by boundary layer dynamics (we won’t speculate on whether this is the case or not), the “true” diurnal patterns would have an even larger amplitude since boundary layer dynamics would result in inverse structures to the observed patterns. Since the observed diurnal (and weekly) patterns of the CSOA factor agree very well with our observations of smoking activities in the vicinity of the sampling site, we are very confident that the patterns presented in Figure 13 reflect the concentrations of smoking-related aerosol well. For this reason we stated in the text:

> P26, L13-19: “The diurnal cycle of the CSOA factor strongly correlates with typical working hours at the measurement location…” and “show distinct differences between working days and weekend, when the administration of the hospital where the measurements took place was closed, supporting the attribution of this PMF factor to locally emitted CSOA.”

For completeness we also provide time series of CSOA and the nicotine tracer ion concentrations in the supplement (Figures S9 and S14).

Comment: (5) the new particle formation in this study appears to have problems too. At least from the average diurnal cycles in Figure 5, we didn’t see “banana” shape. On the other hand, the diurnal cycles appears to indicate strong local sources at both sites.

Reply: Banana-like shapes in time series of particle size distributions are only expected when observing the evolution of the particle size distribution of freshly nucleated particles over time. This can only be done if either the measurement follows the air mass in a Lagrangian experiment or the nucleation occurs over a sufficiently large area simultaneously (like in the boreal forest) and the air masses passing by the measurement site all have the same history. Both are not the case in our measurements, and in similar measurements in urban environments. Therefore it is not surprising that we do not see banana-like shapes in Figure 5 and in the raw data. Also the studies performed by Brines et al. (2015) in the cities of Barcelona, Brisbane, Los Angeles, Madrid, and Rome showed nucleation bursts without strong subsequent growth (depicted in Fig. 5 Brines et al., 2015), different from the typical “banana-like” nucleation episodes usually described in regional background environments. Minguillon et al. (2015) reported the restriction of nucleation events in Barcelona to midday and early afternoon, when condensation sinks are low due to decreased traffic emissions. Therefore, nucleation events found in urban environments are often similar to those found in our study, and do not necessarily exhibit a “banana shape”.

Our measurements were performed stationary in a suburban/urban area, which is why we observe a strong contribution of small particles during the rush hour times in the morning and the evening (of course there are strong local sources near both sites), as discussed in the manuscript (P16, L12-13). During midday, when concentrations of particles from traffic are typically at their minimum, we observe different patterns in the diurnal cycles of particle number concentrations between late fall and late spring. Only during the warmer season we observed increased particle number concentrations during midday. The connection of the increased particle number concentrations during midday with new particle formation events is supported by average particle number size distributions measured with the FMPS. These indicate increased concentrations of rather small particles during this time of the day, as discussed in the manuscript (P16-18).

Comment: (6) the classifications of “home-made” and “advected” might also have large uncertainties. For example, OOA can be from both sources since SV-OOA and LV-OOA cannot be separated. Although nitrate has a shorter life time than sulfate and LV-OOA, many studies have shown that regional transport can be important. I understand the authors can judge this based on the polar plots in Figure 8. In fact, I suggest that the authors re-analyze the polar plots by considering the influences of the number points in each cell. For example, the wind rose plots in Figure 1b shows a small frequency from the northeast, the polar plots in this direction can be significantly biased by sporadic spikes.

Reply: We agree that this classification has large uncertainties. Therefore we described the comparison of “home-made” and “advected” submicron aerosol as a “rough estimate” in the first sentence of the related paragraph (P12, L1). We agree that OOA (not separated into LV- and SV-OOA during Oct/Nov 2013) can be from both, local and remote sources. However, as shown in Figure 7, OOA was found to be rather aged and therefore was assumed to preferentially be associated with the “advected” type. This assumption has some uncertainties and will lead to a small additional uncertainty in the final result of this analysis. However, this small uncertainty is much smaller than the uncertainty implicitly claimed in the text by expressions such as “rough estimate” and “approximately half of the locally measured PM_1 was home-made” (P29, L28). The same is true for potential small fractions of transported nitrate, which also could contribute a slight additional uncertainty to the overall analysis, thereby however partially balancing the potential OOA-related bias.

The referee is right that for the northeast wind direction a relatively low number of data points is available due to the low frequency of wind from this direction. However, an estimation shows that this is not a real problem for our interpretation of the data: According to Figure 1b about 5% of the data are associated with wind from this direction. For ca. 15 days of measurement and 1-minute data this corresponds to about 1080 data points (15 x 24 x 60 x 0.05) for this wind direction. These data points distribute over approximately 90 pixels of the polar plots, resulting in an average of ~12 data points per pixel. Furthermore, in the analysis of the polar plots only the general trends were investigated and not individual “hot spots” of single pixels with extraordinarily high numbers (outliers). Therefore we conclude that even for such wind directions a reasonable data base is available to avoid significant biases by sporadic spikes.

Comment: With this, I cannot recommend it for publication on ACP.

Reply: We hope that after answering to the referee's comments as well as including the requested further information to the manuscript (e.g. discussion of HOA/BC ratios) and adding a supplement with detailed information on the AMS (e.g. comparison of total AMS+BC vs. PM_1 (EDM)) and PMF (e.g. factor time series, factor spectra, comparisons of PMF factors with external tracers) quality assurance, we can overcome the referee's concerns.

Response to anonymous referee #2

We thank anonymous referee #2 for his/her thoughtful and helpful comments. We especially appreciate the suggestions concerning the section on cigarette emissions.

General comments:

The following paper presents a comprehensive study at two different sites of Rome and surroundings (called urban and suburban) for two different seasons, totalizing four rather short datasets. Measurements of coarse and fine aerosol modes were performed, with focus on the latter, as well as several gases and meteorological parameters. Organic aerosol data were further analyzed with PMF and several different components were identified. Overall I recommend the paper if the comments below would be addressed.
Some specific comments, trying not to overlap with the previous Referee:

Specific comments:

1) P7, L21-23: Why Canagaratna et al. (2015) was not used instead?

Reply: Many thanks to the referee for providing that helpful comment. Even if not mentioned, elemental analysis indeed was performed based on the improved-ambient method introduced by Canagaratna et al. (2015). This information was added in the revised manuscript (P7, L22-23).

2) P7, L29-30: What would such variabilities be? Are they inside a 20% variation?

Reply: The variabilities are inside a 20% variation. IE calibrations performed before and after the campaigns in 2013 varied by ~10% (IE: $1.9*10^{-7}$, $1.95*10^{-7,}$ $2.28*10^{-7}$) and we found a variation of ~20% around the average for the IE calibrations performed in 2014 (IE: $1.89*10^{-7}$, $2.64*10^{-7}$). The information on the variability of the IE values for each year was added to the revised manuscript (P7, L30-32):

"Therefore, the observed variability of the IE values (2013: ~10%, 2014: ~20%) is assumed to stem only from the uncertainty of the calibrations, and for each year averages of the determined IE and RIE values were used for data analysis."

3+4) P8, L3-12: More information about the PMF analysis would be very welcome. For example, what was the input matrix size, how many rows and columns? Were the outliers downweighted? Same seasons were run together or separately?

and:

P8, L13-22: The Q/Qexp value is normally useful in the identification of the final solution. However, no information on that was provided.

Reply: In the PMF analysis, each measurement campaign (DIAPASON2013, POPE2013, DIAPASON2014, POPE2014) was evaluated separately. PMF input data were treated as proposed by Ulbrich et al. (2009), as stated at P8, L3-13. M/z with signal-to-noise ratios (SNR) < 0.2 were removed, m/z with 0.2<SNR>2 were downweighted by increasing their error by a factor of 2 and m/z 44-related peaks were downweighted by a factor of sqrt(5).

More information on the PMF analysis (matrix size of the input data, the Q/Q_{exp} values, number of factors for the chosen solution, factor mass spectra, factor and tracer time series) is now provided in the supplementary information.

5) P10, L15-17: It is true that absolute values of POA mass concentration are larger in the suburban area compared to the urban; however, note that the percentages are smaller. According to Figure 2 POA in the urban is still 58% of organics, while suburban is 46%. So it seems to me that POA mass is larger in the suburban because PM1 is 2 times larger and not because BBOA itself. I think those lines need clarification.

Reply: The reviewer is completely right, during 2013 the absolute and the relative contributions of POA-related aerosol at the two sites show an opposite behaviour. This is mainly due to the massive differences in OOA mass concentration measured at the two sites. We assume this OOA is mostly advected, i.e. the observed changes in OOA concentrations between the two sites are due to changes in the histories of the air masses sampled during the different measurement periods, which is also apparent e.g. from the different SO_4 mass concentrations. This change in air mass history, however, should not affect the primary emitted species. Therefore, comparisons of relative POA contributions would be biased by changes in sampled air masses (where OOA absolute mass concentration would change, while POA would not). For the comparison of these locally produced aerosol species, we therefore decided to rather focus on absolute POA concentrations, in order to avoid such an influence of sampled air mass. In order to make the reasoning behind this selection clearer and more transparent we added a brief discussion about this to the revised manuscript (P10, L24-29):

"Note that due to the fact that OOA concentrations are significantly higher in the suburban site in 2013, the relative contribution of POA-related aerosol types (i.e. HOA, COA, and BBOA) is lower at the suburban location during this year. However, in order to avoid a bias in the comparison of the more locally generated POA-related aerosol types by advected aerosol mass, we compare the absolute mass concentrations for the different aerosol types at the different measurement locations/times."

6) Table 3 e Figure 2: Beautiful and instructive figure! Please verify the PM1 values, they do not agree with the Table 3. For instance, Figure 2 says that PM1 at suburban/2013 was 12 µg m-3, while the Table 3 says it was 15±10 µg m-3. Which one is correct? Same thing to the other 3 campaigns.

Reply: The discrepancy between the PM_1 concentrations reported in Table 3 and Figure 2 of the manuscript results from the 2 different measurement instruments these concentrations are based on. PM_1 concentrations presented in the table originate from EDM measurements (optical particle detection), whereas the PM_1 concentrations presented in Figure 2 represent the sum of BC (from MAAP-measurements) and total AMS concentration. The difference in the PM_1 concentrations can arise from the slightly different measurement size ranges or measured particle components, e.g. the AMS+BC PM_1 does not include non-refractory species like Saharan dust, the AMS has a lower cut-off than the EDM, etc. (see discussion in the supplementary material). In the revised manuscript we added a footnote to Table 3, stating that the PM1/2.5/10 values are from EDM measurement. Furthermore, we added also the AMS+BC PM1 concentrations to Table 3 in the revised manuscript and present a comparison of AMS+BC and PM_1 from EDM measurements together with a discussion of the differences in the supplement.

7) P10, L22-25: How can a fresher OOA (so called SV-OOA) be extracted if solar radiation and O3 are larger? Shouldn't it be the opposite? The larger amount of solar radiation and air T should fasten the aerosol ageing. Please provide further explanation. For example, could the fresher OOA be maybe related to different air masses reaching the region during this time of the year, further air circulation/dispersion? Also this time of the year may allow for larger ranges in air T and solar radiation, …

Reply: The reviewer is absolutely right, increased solar radiation and O_3 should result in faster aerosol (and precursor) ageing. This exactly is the reason why during the 2014 measurements precursor material emitted in the greater Rome area are likely sufficiently quickly oxidized to form the fresh SV-OOA before arrival at our measurement site. During the 2013 measurements oxidation processes are slower such that apparently no (or not enough) freshly produced secondary aerosol from precursors from the greater Rome area can be found at the measurement sites but only much more aged material that is transported from further away.

To make this clearer we added the following statement to the revised manuscript (P11, L8-9): "This SV-OOA likely is the result of quick formation of secondary aerosol from precursors originating from the greater Rome area."

8) P10, L27-30: The reduced solar radiation makes a reasonable explanation at the urban site, where OOA increased from 42% to 76% from winter to summer. However, not at the suburban where almost no change was observed (53-56%). That is, if the radiation increased at both sites, why only at the urban such effect was observed? For sure solar radiation is important, but it is not the only aerosol ageing agent. There are locations where LV-OOA is dominant under almost no solar radiation (i.e. Finland). Moreover, was fog observed/measured during the Oct/Nov measurements? Particle water uptake associated

with fog may promote aerosol processing through heterogeneous-phase chemistry. The presence of fog has been well studied in other regions of Italy during the same season (i.e. Po Valley).

Reply: In the lines cited by the reviewer, we stated that the reason for the observation of only a single OOA factor (a rather aged OOA, which is similar to the LV-OOA observed during the spring measurements) in fall is due to the slower processing of precursor material (due to less solar radiation) and therefore reduced production of very fresh oxidized material (see also reply to comment #7). We do not speculate about the reasons for differences or missing differences in absolute concentrations of total oxidized material or their fractional contribution to total (organic) aerosol.

We completely agree that there are other potential factors than solar radiation that could influence the generation of oxidized material. During our measurements we did not observe distinct fog events or other influences which could potentially dominate the formation and aging of OOA.

9) P11, L4-6: The authors say that the lower fraction of sulphate on Oct/Nov could be related to the enhance of POA because of lower boundary layer heights (BLH). If the BLH was lower, that should affect all pollutants equally, right? In addition, a significant change in POA fraction, between seasons, was only observed at the urban site, not in the suburban.

Reply: The idea behind the statement cited by the reviewer is, that while POA is affected by boundary layer height since it is produced locally and mixed only within the boundary layer, transported aerosols (like sulphate or LV-OOA) are not limited to the boundary layer height because during the longer transport time also other mixing processes contribute to their dispersion within the atmosphere. Therefore, changes in boundary layer height will not influence the concentrations of transported aerosols, contrary to those of POA.

To make this clearer we added a short statement to the revised manuscript (P11, L20-24): “Also the relative fraction of sulphate could be lower in Oct/Nov due to an enhanced contribution of primary particles (Table 3) as a consequence of lower boundary layer heights (which limits the dilution of locally produced aerosols while transported aerosols are also diluted by other processes) and, potentially, higher emission strength of local sources during the colder season.”

Regarding the “POA fraction”: The reviewer is right that for the suburban site, the relative fraction of POA-related aerosol in the 2014 measurement (spring) is only slightly lower compared to fall, however, the absolute concentrations of POA-related aerosols are clearly lower. Therefore we changed the term “enhanced fraction” to “enhanced contribution” (see cited text in the previous paragraph).

10) P11, L22-25: The authors say that absolute concentrations of suburban home-made PM1 are larger than urban, probably due to meteorological conditions. Right. However, note that in percentage the urban is larger than the suburban (70 and 47%). In reality, home-made PM1 is smaller in absolute concentrations at the suburban because all PM1 is ~2 times smaller. Thus, the meteorological conditions are the main reason for such decrease in PM1.

The home-made PM1 decrease is just following the PM1 trend. It seems to me that the use of absolute concentrations only, can slightly misguide the reader.

Reply: We agree with the reviewer that due to the large differences in total PM_1 opposite trends between the two measurement sites can be observed for the absolute and relative contributions of home-made aerosol. Since the transported aerosol strongly depends on air mass origin we focused for the discussion of the home-made aerosol on the absolute values only. However, we agree that this could misguide the reader. Therefore, we added the information about the relative concentrations in the revised manuscript (P12, L18-19):
"However, due to the large differences in total PM_1, the relative contribution of home-made PM_1 was higher at the urban location."

11) P13, L6-8: It would be very kind of the authors to point out in here which minerals were identified in Silvia Nara, personal communication 2016, since this communication is not easily available.

Reply: We completely agree with the referee that this information is not easily available and therefore added it to the revised manuscript (P13, L32-P14, L3). Furthermore, we are now able to replace the personal communication with a reference to a manuscript in preparation:

"PIXE analysis of 1-hour filter samples confirmed a significant increase of mineral dust concentrations (i.e. Na, Mg, Si, Al, Ti, K, Ca, Fe; Nava et al., 2012) at ground level during the identified dust periods (Barnaba et al., in preparation 2016)."

12) P18, L16-20: In fact, what Jimenez et al. (2009) state is that the larger dynamic range in solar radiation and air temperature may cause the different OOAs.

Reply: Thanks for the comment. We have clarified this in the revised manuscript (P19, L26-30):

"This is typically only observed during summer conditions, when the dynamic range of temperature, ozone concentration and solar radiation is large, which is assumed to be the main driving force for the variability of the OOA volatilities (Jimenez et al., 2009)."

13) P19, L23-28: Those last sentences are slightly confusing and seem to contradict the "home-made vs advected" section of this study. That is, in the "home-made vs advected" section nitrate was considered home-made. Here it is said that nitrate is north-east advected. Please clarify. Why are those sections separated if they complement one another?

Reply: Thank you for pointing this out. Actually, there is no contradiction but simply unfortunate wording in this sentence. We did not mean that nitrate is long-range transported from north-easterly directions, but that NO_3 was elevated when wind was from this direction, indicating sources for this aerosol component being located preferentially in this direction. We re-worded the respective sentence in order to make this clearer (P21, L6-8):

“Elevated NH_4 and SO_4 concentrations were mainly measured during times with south-westerly wind direction, whereas for NO_3 rather an increase for north-easterly directions was observed.”

14) P21, L7-11: I’m surprised BBOA is still so significant in late spring. Unfortunately, the authors did not provide the MS for the reader. Are the two BBOAs (summer-like and winter-like) similar? If one BBOA was more related to agricultural and the other to agricultural and domestic heating, I’d expect to see some differences among them, was any observed? Also with respect to external tracers.

Reply: We observed agricultural burning activities during both, the late autumn and the late spring measurements. Due to the relatively mild conditions also during the Oct/Nov 2013 measurements, we do not expect strong contributions from domestic heating also during this season. To make this point clearer we added the following statement to the revised manuscript: (P21, L27-29)

“However, due to the moderate temperatures also during the Oct/Nov 2013 measurements, we do not expect strong contributions from domestic heating.”

Furthermore, we have included the BBOA spectra and time series (also of the external tracers) in the new supplement. The spectra of BBOA measured during the two different seasons show clear differences, but it was not possible to identify any relations to different BBOA sources or transformation processes. Actually, for DIAPASON2013 the final PMF solution contained two factors indicating BBOA. We examined both BBOA factors in order to identify indications of different sources/processes. Since the time series of both BBOA factor spectra were quite similar (see Fig. S7) and the most dominant event of biomass burning (see P21, L31-33) was included in both BBOA factor time series, we are confident that both BBOA factors represent aerosol from the same sources and are only the result of splitting within the PMF analysis. This is also presented in the supplementary information.

15) P24, L1-4: Very interesting! The MS of CSOA identified by this study look quite different from the previous (Fröhlich et al., 2015 and Faber et al., 2013), with prominent fragments at m/zs 84. Also the N-containing fragment at m/z 42 look prominent and present in NIST MS database. Why this fragment was not mentioned in this study? Was it because of interference from other fragments in the same nominal m/z?

Reply: We are grateful to the referee for this very interesting and helpful comment. In fact, the N-containing ion at m/z 42 ($C_2H_4N^+$) shows very similar time series (R^2>0.8) to the CSOA factor as well as to the here proposed nicotine marker ion $C_5H_{10}N^+$. This ion $C_2H_4N^+$ is significantly more prominent in the CSOA spectra ($fC_2H_4N^+$ =1-2%) compared to all the other PMF factor spectra ($fC_2H_4N^+$ = 0.1-0.6%). However, even in the DIAPASON data, which are not affected by cigarette emissions, the variation of the concentration of this ion is quite strong, showing that this ion is not as specific to cigarette emissions as the ion at m/z 84. Therefore, it is not easy to define a criterion (e.g. a detection limit based on the POA concentration) for this ion in order to identify cigarette smoke affected data.

However, the combination of information from both ions strengthens the association of a PMF factor to cigarette emissions. Therefore, we have provided some information on that ion and a discussion of its applicability as a CSOA tracer in the revised manuscript (P25, L11; P25, 24-29; P27, L18-25; P28, L1-6).

16) P24, L5-6: Just a comment: when comparing SV-OOA and LV-OOA MS from the AMS database (Ng et al., 2010), also a R2=0.65 is obtained, and those are very different things! Thus, I'd be very careful in comparing CSOA obtained in this study to previous ones. I mean, there is no need to try to make them look similar, since the current study seems to have identified a much clearer CSOA factor.

Reply: Thank you for this hint. We completely agree that an R^2 of 0.65 can result from the comparison of very different types of mass spectra. The point of presenting this information is rather to show the variability that can occur in the identification of CSOA factors in different data sets.

17) P25, L3: The authors used C5H10N+ fragment as a marker for CSOA. Since the measurements were performed with and HR-ToF-AMS, which provides size distribution data. Did the authors try to identify the size distribution of the CSOA using this same marker? Or perhaps just UMR m/z 84, 42?

Reply: Thanks to the referee for this suggestion. We did not save HR size distribution data, so it is not possible to extract the ion's size distributions separately. Unfortunately also the signal-to-noise ratio of the individual UMR size distributions for m/z 84 and 42 is not sufficient to provide distinct information on the CSOA particle sizes. Therefore we did not further analyse them for this purpose.

18) P18, L4: The right citation is Alfarra et al., 2004 (Characterization of urban and rural organic particulate in the Lower Fraser Valley using two Aerodyne Aerosol Mass Spectrometers).

Reply: Thanks for the comment. We have changed this reference in the revised manuscript.

19) P18, L5-11: This sentence is too long and difficult to read.

Reply: Thank you for this hint. We replaced the original sentence: "Under conditions where sufficient freshly oxidised organic aerosol is available in the ambient air, PMF can separate the OOA into two factors associated with mass spectra containing different relative fractions of *m/z* 44 and *m/z* 43 (f44 and f43, ratio of *m/z* 44 and *m/z* 43 signal, respectively, to the total signal of organics): (I) A less oxidised, fresher, more locally produced semi-volatile OA (SV-OOA) associated with higher f43, and (II) a stronger oxidised, more aged low-volatile OA (LV-OOA) associated with higher f44 (Ng et al., 2010)."

with: "Under conditions where sufficient freshly oxidised organic aerosol is available in the ambient air, PMF can separate the OOA into two factors. These factors differ in their relative fractions of *m/z* 44 and *m/z* 43 (f44 and f43, ratio of *m/z* 44 and *m/z* 43 signal, respectively, to the total signal of organics), which reflects their different degrees of oxidation. The factor associated with higher f43 indicates a less oxidised, fresher, more locally produced semi-volatile OA (SV-OOA), whereas a higher f44 indicates a stronger oxidised, more aged low-volatile OA (LV-OOA) (Ng et al., 2010)."

20) P20, L14: Probably the ":" should be replaced by a ".".

Reply: When replacing the ":" by a "." the meaning would be changed. Since the original version was apparently not clear, we changed it to:

"This event was used during the identification of the PMF solution since only a factor including this event could be considered to be attributed to biomass burning emissions."

21) P23, L13: Replace ":" by ".".

Reply: The referee's suggestion was applied in the revised manuscript.

Response to anonymous referee #3

We thank anonymous referee #3 for his/her helpful comments.

General comments:

This paper describes measurements from campaigns in and around Rome during different seasons. It predominantly considers HR-AMS data but also incorporates estimates of Saharan dust convection and aerosol size distribution. It offers valuable insights relating to the impact of different sources on PM1 in urban areas in Europe and builds on my previous studies. It makes particular advances in the consideration of cigarette smoke and its measurement using HR-AMS. As with many short seasonal campaigns it is difficult to draw firm conclusions due to the large variation in meteorological conditions, however, the authors have contrasted different seasons without over-interpreting.

Specific comments:

Comment: Specific Comments Labelling NO3 as 'home made' (pg 11 line 16). Although the formation of NO3 from gaseous precursors occurs over a short time scale and will be partially 'home made', it is affected over large distances and a portion is likely to be advected. This will impact on your % estimates and should be discussed and altered appropriately.

Reply: Thank you for pointing this out. We completely agree that nitrate can also be transported and consequently contributing to the "advected" aerosol. Since the total nitrate fraction is very low (4-7%) this will result only in a small error in the total percentage of “advected” and “home-made” aerosol. We now discuss this briefly in the revised manuscript (P12, L7-13):

“While nitrate is formed quickly and thus strongly contributes to the “home-made” aerosol fraction, it can also be transported. The resulting fraction of “home-made” might therefore be slightly biased high, however by a few percent at most due to the small total contribution of nitrate to PM_1. For the POPE2013 measurements OOA shows only poor correlations with SO_4, but slightly better with NO_3, suggesting either a local contribution of OOA or the transport of NO_3. Whatever the case may be, it will contribute to the error of the estimation.”

Comment: Two modes in particle size distribution (pg 14 line 1). The second ’peak’ in size distribution at 0.6 um may be an influence of reduced counting efficiency to aerosols in this size range.

Reply: We agree that for the first channel of the APS reduced counting efficiency could result in biased results. However, this should not be the case for the larger size channels. Since the second peak around 0.6 µm distributes over several size channels and since we also observe increased concentrations in this size range in the OPC data and increased PM_1 concentrations in the EDM during the dust event, we are quite confident that this mode is not only an artefact due to reduced counting efficiency.

Comment: Bivariate polar plots (Fig 8) NH4 is reported for 2013 but not 2014.

Reply: The polar plot of NH_4 for DIAPASON2014 was added to the revised manuscript. It was only omitted in the first version of the manuscript in order to avoid graphical unbalance.

We also added a short discussion on it (P20, L29-32):

“The polar plot of NH_4 shows a hot spot at low wind speeds in northern direction, which is also reflected in the patterns of SV-OOA and NO_3. Increased NH_4 concentrations are also observed at higher wind speeds in south-westerly direction, agreeing with the polar plot patterns of LV-OOA and SO_4.”

Comment: Technical Comments pg 11 line 4 ’lowered’ should read ’lower’

Reply: Done, thank you.

Comment: pg 12 line 3 ’always was’ should read ’was always’

Reply: Done, thank you.

Comment: Table 5 ’PM10 in PM1’ should read ’PM1 in PM10’

Reply: Table 5 was changed. We now present the absolute PM_1 concentrations and the contribution of PM_1 to PM_{10}.

Comment: Pg 17 line 19-20 'probably less precursors are' should read 'lower concentrations of precursors are probably' and 'more precursors' should read higher concentrations of precursors

Reply: Thank you for pointing this out. We changed: "At this measurement location, probably less precursors are available than in central Rome, but more precursors than at a remote regional background site such as in the study of Costabile…"

to: "At this measurement location, probably lower concentrations of precursors are available than in central Rome, but higher concentrations than at a remote regional background site such as in the study of Costabile…".

Comment: Pg 19 line 26 'aging level' should read 'degree of aging'

Reply: We replaced: "Based on the polar plot characteristics no consistent trend indicating the aging level, the source or the formation process…"

with: "Based on the polar plot characteristics no consistent trend indicating the degree of aging, the source or the formation process…".

References

Barnaba, F., Bolignano, A., Di Liberto, L., Morelli, M., Lucarelli, F., Nava, S., Perrino, C., Canepari, S., Basart, S., Costabile , F., Dionisi, D., Ciampichetti, S., Sozzi, R., and Gobbi, G. P.: Desert dust contribution to PM10 levels in Italy: results from an automated method building on and upgrading the relevant European Commission Guidelines in support to the Air Quality Directive 2008/50, in preparation 2016.

Brines, M., Dall'Osto, M., Beddows, D. C. S., Harrison, R. M., Gomez-Moreno, F., Nunez, L., Artinano, B., Costabile, F., Gobbi, G. P., Salimi, F., Morawska, L., Sioutas, C., and Querol, X.: Traffic and nucleation events as main sources of ultrafine particles in high-insolation developed world cities, Atmos. Chem. Phys., 15, 5929-5945, 2015.

Canagaratna, M. R., Jimenez, J. L., Kroll, J. H., Chen, Q., Kessler, S. H., Massoli, P., Ruiz, L. H., Fortner, E., Williams, L. R., Wilson, K. R., Surratt, J. D., Donahue, N. M., Jayne, J. T., and Worsnop, D. R.: Elemental ratio measurements of organic compounds using aerosol mass spectrometry: characterization, improved calibration, and implications, Atmos. Chem. Phys., 15, 253-272, 2015.

Crippa, M., DeCarlo, P. F., Slowik, J. G., Mohr, C., Heringa, M. F., Chirico, R., Poulain, L., Freutel, F., Sciare, J., Cozic, J., Di Marco, C. F., Elsasser, M., Nicolas, J. B., Marchand, N., Abidi, E., Wiedensohler, A., Drewnick, F., Schneider, J., Borrmann, S., Nemitz, E., Zimmermann, R., Jaffrezo, J. L., Prevot, A. S. H., and Baltensperger, U.: Wintertime aerosol chemical composition and source apportionment of the organic fraction in the metropolitan area of Paris, Atmos. Chem. Phys., 13, 961-981, 2013a.

Crippa, M., El Haddad, I., Slowik, J. G., DeCarlo, P. F., Mohr, C., Heringa, M. F., Chirico, R., Marchand, N., Sciare, J., Baltensperger, U., and Prevot, A. S. H.: Identification of marine and continental aerosol sources in Paris using high resolution aerosol mass spectrometry, J. Geophys. Res.-Atmos., 118, 1950-1963, 2013b.

Faber, P., Drewnick, F., Veres, P. R., Williams, J., and Borrmann, S.: Anthropogenic sources of aerosol particles in a football stadium: Real-time characterization of emissions from cigarette smoking, cooking, hand flares, and color smoke bombs by high-resolution aerosol mass spectrometry, Atmos. Environ., 77, 1043-1051, 2013.

Jimenez, J. L., Canagaratna, M. R., Donahue, N. M., Prevot, A. S. H., Zhang, Q., Kroll, J. H., DeCarlo, P. F., Allan, J. D., Coe, H., Ng, N. L., Aiken, A. C., Docherty, K. S., Ulbrich, I. M., Grieshop, A. P., Robinson, A. L., Duplissy, J., Smith, J. D., Wilson, K. R., Lanz, V. A., Hueglin, C., Sun, Y. L., Tian, J., Laaksonen, A., Raatikainen, T., Rautiainen, J., Vaattovaara, P., Ehn, M., Kulmala, M., Tomlinson, J. M., Collins, D. R., Cubison, M. J., Dunlea, E. J., Huffman, J. A., Onasch, T. B., Alfarra, M. R., Williams, P. I., Bower, K., Kondo, Y., Schneider, J., Drewnick, F., Borrmann, S., Weimer, S., Demerjian, K., Salcedo, D., Cottrell, L., Griffin, R., Takami, A., Miyoshi, T., Hatakeyama, S., Shimono, A., Sun, J. Y., Zhang, Y. M., Dzepina, K., Kimmel, J. R., Sueper, D., Jayne, J. T., Herndon, S. C., Trimborn, A. M., Williams, L. R., Wood, E. C., Middlebrook, A. M., Kolb, C. E., Baltensperger, U., and Worsnop, D. R.: Evolution of Organic Aerosols in the Atmosphere, Science, 326, 1525-1529, 2009.

Kostenidou, E., Florou, K., Kaltsonoudis, C., Tsiflikiotou, M., Vratolis, S., Eleftheriadis, K., and Pandis, S. N.: Sources and chemical characterization of organic aerosol during the summer in the eastern Mediterranean, Atmos. Chem. Phys., 15, 11355-11371, 2015.

Minguillon, M. C., Brines, M., Perez, N., Reche, C., Pandolfi, M., Fonseca, A. S., Amato, F., Alastuey, A., Lyasota, A., Codina, B., Lee, H. K., Eun, H. R., Ahn, K. H., and Querol, X.: New particle formation at ground level and in the vertical column over the Barcelona area, Atmospheric Research, 164, 118-130, 2015.

Nava, S., Becagli, S., Calzolai, G., Chiari, M., Lucarelli, F., Prati, P., Traversi, R., Udisti, R., Valli, G., and Vecchi, R.: Saharan dust impact in central Italy: An overview on three years elemental data records, Atmos. Environ., 60, 444-452, 2012.

Ng, N. L., Canagaratna, M. R., Zhang, Q., Jimenez, J. L., Tian, J., Ulbrich, I. M., Kroll, J. H., Docherty, K. S., Chhabra, P. S., Bahreini, R., Murphy, S. M., Seinfeld, J. H., Hildebrandt, L., Donahue, N. M., DeCarlo, P. F., Lanz, V. A., Prevot, A. S. H., Dinar, E., Rudich, Y., and Worsnop, D. R.: Organic aerosol components observed in Northern Hemispheric datasets from Aerosol Mass Spectrometry, Atmos. Chem. Phys., 10, 4625-4641, 2010.

Ortega, A. M., Hayes, P. L., Peng, Z., Palm, B. B., Hu, W. W., Day, D. A., Li, R., Cubison, M. J., Brune, W. H., Graus, M., Warneke, C., Gilman, J. B., Kuster, W. C., de Gouw, J., Gutierrez-Montes, C., and Jimenez, J. L.: Real-time measurements of secondary organic aerosol formation and aging from ambient air in an oxidation flow reactor in the Los Angeles area, Atmos. Chem. Phys., 16, 7411-7433, 2016.

Sun, Y., Du, W., Fu, P., Wang, Q., Li, J., Ge, X., Zhang, Q., Zhu, C., Ren, L., Xu, W., Zhao, J., Han, T., Worsnop, D. R., and Wang, Z.: Primary and secondary aerosols in Beijing in winter: sources, variations and processes, Atmos. Chem. Phys., 16, 8309-8329, 2016.

Ulbrich, I. M., Canagaratna, M. R., Zhang, Q., Worsnop, D. R., and Jimenez, J. L.: Interpretation of organic components from Positive Matrix Factorization of aerosol mass spectrometric data, Atmos. Chem. Phys., 9, 2891-2918, 2009.

Xu, L., Williams, L. R., Young, D. E., Allan, J. D., Coe, H., Massoli, P., Fortner, E., Chhabra, P., Herndon, S., Brooks, W. A., Jayne, J. T., Worsnop, D. R., Aiken, A. C., Liu, S., Gorkowski, K., Dubey, M. K., Fleming, Z. L., Visser, S., Prevot, A. S. H., and Ng, N. L.: Wintertime aerosol chemical composition, volatility, and spatial variability in the greater London area, Atmos. Chem. Phys., 16, 1139-1160, 2016.

Zhang, J. K., Sun, Y., Liu, Z. R., Ji, D. S., Hu, B., Liu, Q., and Wang, Y. S.: Characterization of submicron aerosols during a month of serious pollution in Beijing, 2013, Atmos. Chem. Phys., 14, 2887-2903, 2014.

Zhang, Q., Jimenez, J. L., Canagaratna, M. R., Ulbrich, I. M., Ng, N. L., Worsnop, D. R., and Sun, Y.: Understanding atmospheric organic aerosols via factor analysis of aerosol mass spectrometry: a review, Anal. Bioanal. Chem., 401, 3045-3067, 2011.

Zhang, Y. J., Tang, L. L., Wang, Z., Yu, H. X., Sun, Y. L., Liu, D., Qin, W., Canonaco, F., Prevot, A. S. H., Zhang, H. L., and Zhou, H. C.: Insights into characteristics, sources, and evolution of submicron aerosols during harvest seasons in the Yangtze River delta region, China, Atmos. Chem. Phys., 15, 1331-1349, 2015.

Atmospheric aerosols in Rome, Italy: Sources, dynamics and spatial variations during two seasons

Caroline Struckmeier[1], Frank Drewnick[1], Friederike Fachinger[1], Gian Paolo Gobbi[2] and Stephan Borrmann[1, 3]

[1]{Particle Chemistry Department, Max Planck Institute for Chemistry, Mainz, Germany}

[2]{Institute of Atmospheric Sciences and Climate, ISAC-CNR, Roma, Italy}

[3]{Institute for Atmospheric Physics, Johannes Gutenberg University, Mainz, Germany}

Correspondence to: C. Struckmeier (c.struckmeier@mpic.de), F. Drewnick (frank.drewnick@mpic.de)

Abstract

Investigations on atmospheric aerosols and their sources were performed during October/November 2013 and May/June 2014 subsequently in a suburban area of Rome (Tor Vergata) and in central Rome (near St. Peter's Basilica). During both years a Saharan dust advection event temporarily increased PM_{10} concentrations at ground level by ~~approximately 10~~some 12-17 µg m^{-3}. Generally, during Oct/Nov the ambient aerosol was more strongly influenced by primary emissions, whereas higher relative contributions of secondary particles (sulphate, aged organic aerosol) were found during May/June. Absolute concentrations of anthropogenic emission tracers (e.g. NO_x, CO_2, particulate polyaromatic hydrocarbons, traffic-related organic aerosol) were generally higher at the urban location. Positive matrix factorisation was applied to the PM_1 organic aerosol (OA) fraction of aerosol mass spectrometer (HR-ToF-AMS) data in order to identify different sources of primary OA (POA): traffic, cooking, biomass burning, and (local) cigarette smoking. While biomass burning OA was only found at the suburban site, where it accounted for the major fraction of POA (18-24 % of total OA), traffic and cooking were more dominant sources at the urban site. A particle type associated with cigarette smoke emissions, which is associated with a potential characteristic marker peak (*m/z* 84, $C_5H_{10}N^+$, a nicotine fragment) in the mass spectrum, was only found in central Rome, where it was emitted in close vicinity to the measurement location. Regarding secondary OA, in Oct/Nov, only a very aged, regionally advected oxygenated OA was found, which contributed 42-53 % to the total OA. In May/June total oxygenated OA accounted for 56–76 % of the OA. Here also a fraction (18-26 % of total OA) of a fresher, less oxygenated OA of more local origin was observed. New particle formation events were identified from measured particle number concentrations and size distributions during May/June 2014 at both sites. While they were observed every day at the urban location, at the suburban location they were only found under favourable meteorological conditions, but independent of advection of the Rome emission plume. Particles from sources in the metropolitan area of Rome and particles advected from outside Rome contributed 42-70 % and 30-58 % to total measured PM_1, respectively. Apart from the general aerosol characteristics, in this study the properties (e.g. emission strength) and dynamics (e.g. temporal behaviour) of each identified aerosol type is investigated in detail in order to provide a better understanding of the observed seasonal and spatial differences.

1 Introduction

Atmospheric aerosol particles remain a major uncertainty in both, estimations of climate change (Boucher et al., 2013) and of impact of air pollution on public health (Heal et al., 2012), and therefore are a major topic of current research (Fuzzi et al., 2015). Identifying the sources, properties and concentrations of atmospheric particles is essential for evaluating their effect on climate and health and constitutes a crucial step in finding measures for the improvement of air quality.

Many studies on aerosols and their sources have been performed in urban environments (e.g. Freutel et al., 2013; Mohr et al., 2012; Zheng et al., 2005), which are characterized by high population densities and a large diversity of particle sources. Typical urban aerosol sources include road traffic, cooking, and heating activities. Also emissions from biomass burning can be important, both of regional origin (e.g. agricultural and wild fires; Reche et al., 2012), and from residential wood combustion, which recently has become more prominent in Europe even in urban environments (Fuller et al., 2013).

Many of these anthropogenic sources emit large amounts of organic material in the fine particle fraction (e.g. Hildemann et al., 1991). In recent studies of particle source identification (e.g. Allan et al., 2010; Mohr et al., 2012; Reche et al., 2012), positive matrix factorisation (PMF) was applied to separate the organic aerosol (OA) fraction into different factors associated with various OA sources, thereby providing indications about the fraction of primary and secondary organic aerosol (POA and SOA) (Zhang et al., 2011). Oxygenated organic aerosol (OOA), mainly associated with SOA, is typically found to be the most abundant fraction of OA (Lanz et al., 2010), with concentrations depending on season and location (Zhang et al., 2011). Several studies, mainly such from observations during summer time (Lanz et al., 2010), show discrimination of OOA into a fresher and a more aged type of OOA based on different states of oxygenation and/or volatility (Jimenez et al., 2009).

While AMS measurements yield useful information on the age of OA, they cannot provide evidence for new particle formation of fresh secondary aerosol. Indications for such, however, can be found in physical aerosol properties like particle number concentration or size distributions (e.g. Alam et al., 2003). New particle formation events in urban environments have been investigated previously in several studies (e.g. Alam et al., 2003; Brines et al., 2015; Minguillon et al., 2015; Shi et al., 2001; Zhang et al., 2004), and especially in the early afternoon seem to be responsible for elevated particle number concentrations in urban areas in Southern Europe (Reche et al., 2011).

On the other hand, while the health impact of coarse particles (PM_{10}-$PM_{2.5}$) is not yet fully understood (Heal et al., 2012), the association between Saharan dust advections and mortality/hospitalisation is quite well demonstrated (Stafoggia et al., 2016). Deserts are large sources for mineral dust, which can strongly contribute to atmospheric PM_{10} levels, especially in Southern Europe. Measurements performed in the period 2001-2004 during Saharan dust advections over Rome showed a mean Saharan dust contribution of 12-16 $\mu g\ m^{-3}$ to daily PM_{10} concentrations, leading to an average annual increase of about 2 $\mu g\ m^{-3}$ (Gobbi et al., 2013). In the central Mediterranean region, maximum dust concentrations are typically observed from spring to autumn (Barnaba and Gobbi, 2004).

In this study, we investigate the occurrence and properties of ambient aerosol from different types of sources in Rome, which apart from local emissions can be influenced by advected aerosol from continental Europe and the Sahara desert. During two different seasons (Oct/Nov 2013 and May/June 2014) and at two different locations (city centre and suburb), stationary measurements of chemical and physical properties of aerosols, several trace gases, and meteorological variables were performed. Non-refractory components of submicron particles were measured with an Aerodyne high-resolution time-of-flight aerosol mass spectrometer (HR-ToF-AMS). To support identification of particle sources, their strength and temporal behaviour, the OA measured with the HR-ToF-AMS was further separated into different factors using PMF.

Based on these measurements, in this work the urban atmosphere of Rome is investigated in terms of particle source identification with a special focus on seasonal and spatial differences influencing the presence and/or the characteristics of aerosol types in the city area.

2 Experimental

2.1 Measurement locations and periods

Measurement results presented in this study were obtained during four intensive field campaigns in the greater Rome area, Italy (Table 1). The city of Rome covers an area of 1300 km^2 and has a population of about 2.9 million residents (about 4.3 million residents within the whole metropolitan area of 5350 km^2). Three airports are located in the Rome province, including the largest one in Italy (Fiumicino). Heavy industries are not found in Rome; the economy is mainly based on services, education, construction, tourism, etc. Parks and gardens cover some 34 % of the city area. Rome is characterised by high traffic volume and density: about 50 % of the population commutes every day, mainly by private cars. The cars per capita ratio in the city is 550 per 1000 inhabitants.

Measurements referred to as DIAPASON were performed during Oct/Nov 2013 and May/June 2014 at the Institute of Atmospheric Sciences and Climate (CNR-ISAC) in Tor Vergata, Rome. The institute is located in the south-eastern outskirts of ~~Rome~~the city (41°50’30.2’’N, 12°38’51.2’’E, 103 m a.s.l., 14 km from central Rome) and considered as an urban background site. The measurement platform MoLa (see Sect. 2.2) was positioned at a free field with no buildings within a radius of 200 m. A frequently used street is located at approximately 100 m distance in northern direction. The closest highway (A1) is situated south-westerly at a distance of about 700 m. Single-house ~~villages~~suburbs are scattered over this territory, starting some 1 km from the site. Frascati, a town on the Alban Hills, is located at about 4 km distance in south-easterly direction. During both periods measurements at Tor Vergata were supported by the EC-LIFE+ project DIAPASON (Desert-dust Impact on Air quality through model-Predictions and Advanced Sensors ObservatioNs), which aims on improving existing tools to assess the contribution of Saharan dust to local PM$_{10}$ levels (http://www.diapason-life.eu/, last access ~~09.05~~11.11.2016). For this reason measurements were scheduled in periods where a dust advection event could be expected and was forecasted by a number of dust forecasts such as the DREAM8b (Basart et al., 2012), the SKIRON (Kallos et al., 1997) and the Tel Aviv University (Alpert et al., 2002) models.

The “POPE” (Particle Observations around St. PEter’s) measurement campaigns were conducted during November 2013 and June 2014 in central Rome. Measurements were performed inside a courtyard belonging to the administration of the hospital “Santo Spirito” (41°54'04.3"N, 12°27'41.5"E, 18 m a.s.l.), which is positioned approximately 600 meters from St. Peter’s Basilica. This urban measurement site is surrounded by highly frequented streets, separated from the courtyard by the four-storey building of the hospital. The surrounding area is a touristic hotspot with frequent religious gatherings (e.g. festivals, masses) and many restaurants and shops. Especially on Wednesdays during the papal audience and on Sundays, if the masses are held at St. Peter’s or during papal speeches (Angelus), the area attracts numerous visitors.

The distance between the two measurement sites is around 17 km. During both years measurements at Tor Vergata and central Rome were performed subsequently.

2.2 Instrumentation

All measurements were performed with the **Mo**bile aerosol research **La**boratory MoLa (Drewnick et al., 2012). MoLa is based on a regular Ford Transit delivery vehicle equipped with instruments for on-line measurements of chemical and physical properties of aerosols, important trace gases and meteorological variables (Table 2). Further description as well as details of the aerosol inlet system can be found in Drewnick et al. (2012). All results presented in this study were obtained in stationary measurements, with the aerosol inlet and a meteorological station at 7 m above ground level.

An HR-ToF-AMS (Aerodyne Research, Inc.; DeCarlo et al., 2006) was used to measure particulate mass concentrations of submicron non-refractory organics (“Org”), sulphate (“SO_4”), nitrate (“NO_3”), ammonium (“NH_4”) and chloride (“Chl”). The HR-ToF-AMS allows the distinction between different ions at the same nominal mass-to-charge-ratio (*m/z*). The instrument was run in V-mode, i.e. the ions followed a “V”-shaped trajectory through the mass spectrometer, allowing high sensitivity at slightly lower mass resolution, compared to the higher resolution mode (W-mode).

In the framework of the EC-LIFE+ project DIAPASON additional measurements were performed at the Tor Vergata measurement site, which aimed at assessing the contribution of Saharan dust to PM levels. These measurements included hourly PM_{10}, a three-wavelength nephelometer, one-hour filter sampling for off-line PIXE analysis (Lucarelli et al., 2014) and a polarization LIDAR-ceilometer for the assessment of presence, phase and altitude of aerosol layers (Gobbi et al., 2004). Boundary layer heights were determined from polarisation LIDAR-ceilometer measurements based on the method described by Angelini and Gobbi (2014).

Since the POPE measurements were performed inside a courtyard~~,~~ surrounded by four-storey tall buildings, wind speed, wind direction and solar radiation data are affected and not used for these periods. The time resolution for all measurements is 60 s or better.

3 Data preparation and analysis

3.1 General data analysis

All measured variables were corrected for sampling delays and set on a common 1-second time base. Particle losses during the transport through the inlet system were negligible (Drewnick et al., 2012). The data time series were carefully inspected and quality checked. Data affected by instrument calibrations and malfunctions were removed. Measurement periods influenced by local emissions (e.g. moving vehicles in the immediate vicinity of MoLa) were identified based on prominent short peaks in the time series of CO_2 and particle number concentration (PNC) which significantly exceeded the typical variability, and removed from the data set. After data decontamination, 5-minute averages were calculated for all variables, which were used for all following analyses if not otherwise indicated.

Data collected during the DIAPASON2013/POPE2013 and DIAPASON2014/POPE2014 field campaigns are presented in local winter (UTC+1) and local summer (UTC+2) time, respectively. For convenience, DIAPASON2013 data are presented only in winter time, even though the change from summer to winter time was at the fifth day of measurements (27.10.2013). This means data measured prior to the time change is 1 hour shifted to the past with respect to local (summer) time. Especially diurnal patterns dominated by anthropogenic activity patterns (e.g. traffic during rush hour times) could be affected by ignoring the time change. In order to evaluate this possible influence, diurnal cycles measured before and after the time change were compared, but no significant shift of diurnal patterns was observed between the two time periods. Since diurnal cycles are not only modulated by the source emission strengths, but also by boundary layer dynamics, we assume the missing evidence of the time shift in the data is caused by a combination of influence from boundary layer dynamics and the temporal uncertainty of diurnal cycles calculated over only a few days. Additionally, anthropogenic activities could have partially not been instantly adapted to the time change, which would lead to a blurring of the effect of the time change on diurnal cycles.

Polar plots of species concentration as a function of local wind direction and wind speed were generated by averaging species concentrations (60 s data) into bins of 5° wind direction and 0.5 m s^{-1} wind speed. The resulting data were smoothed by applying a natural neighbour interpolation (Sibson, 1981). As presented by Yu et al. (2004), such polar plots can provide directional information on sources in the vicinity of a monitoring site. Sources close to the measurement site are typically indicated by concentration decreases with increasing wind speed, while pollutants which are emitted from remote sources or at higher altitudes need higher wind speeds to be transported to the monitoring site (Yu et al., 2004). Similarly, Carslaw et al. (2006) reported the capability of such bivariate polar plots to distinguish between no-buoyancy sources like traffic (decreased pollutant concentration with increasing wind speed) and buoyant plumes emitted from sources like chimney stacks (increased concentrations with increasing wind speed), where the plume needs to be brought down to ground-level from a higher altitude.

3.2 HR-ToF-AMS data analysis

AMS data evaluation was performed within Igor Pro 6.37 (Wavemetrics) with the standard AMS data analysis software SQUIRREL 1.55H and PIKA 1.14H. Elemental ratios calculated from organic ion fragments (Aiken et al., 2007) based on the improved calibration method (Canagaratna et al., 2015) were determined using APES light 1.06 (all available at http://cires1.colorado.edu/jimenez-group/ToFAMSResources/ToFSoftware/). For all data sets a collection efficiency of 0.5 was applied, which is typical for the given ambient measurement conditions (Canagaratna et al., 2007). The ionisation efficiency (IE) of the ion source and the relative ionisation efficiency (RIE) for ammonium and sulphate (e.g. Canagaratna et al., 2007) were determined before the DIAPASON and after the POPE campaigns in both years. An additional IE calibration in 2013 after the field measurements showed no general trend in IE values. Therefore, the observed variability of the IE values (2013: ~10 %, 2014: ~20 %) is assumed to stem only from the uncertainty of the calibrations, and for each year averages of the determined IE and RIE values were used for data analysis. Measurements of particle free air were carried out multiple times during the campaigns and were used for correction of instrumental background effects.

In order to separate total OA into different aerosol types, PMF (Paatero and Tapper, 1994; Ulbrich et al., 2009) was applied to high-resolution mass spectra of the OA fraction with *m/z* below 131. This was done separately for each measurement campaign. The procedure of HR data and error matrices (matrix input sizes can be found in the supplement) preparation is described in detail in DeCarlo et al. (2010). Isotopes constrained to a fractional signal of their parent ion were excluded from the analysis. Within the PMF Evaluation Tool- v2.06 ions with signal-to-noise ratio < 0.2 were removed from data and error matrices, and ions with signal-to-noise ratio between 0.2 and 2 were down-weighted in the analysis by increasing their estimated error by a factor of two (Ulbrich et al., 2009). Particulate CO_2^+ (*m/z* 44) and its associated ions at *m/z* 16, 17, 18 and 28 were down-weighted by a factor of $\sqrt{5}$ (Ulbrich et al., 2009, supplemental information).

In order to find the most reasonable and robust PMF solution, the number of factors (one up to ten, always at least two more than the finally selected solution), the rotational force parameter (fPeak: -1 to 1; Δ = 0.~~1~~2) and the starting point (seed: 0 to 50; Δ = 1) were varied (see Ulbrich et al., 2009 for methodological details). Solutions with fPeak=0 and seed=0 turned out to yield robust results for all data sets. The evaluation of potential PMF solutions was based on comparisons of the resulting factor time series with those of co-located measurements (see Sect. 4.2), and of factor mass spectra with such from the literature. Residues, i.e. the contribution of organic mass concentrations not included in any of the factors, accounted for <1 % of the organics mass concentration in all used PMF solutions and are therefore negligible. Mass spectra and time series of each identified PMF factor can be found in the supplement.

4 Results and discussion

4.1 Overview: Differences between seasons and locations

This section provides a broad overview of the mean conditions of local meteorology and air quality during each measurement campaign (Table 3, Fig. 1), and discusses their seasonal and spatial differences. Figure 2 provides an overview of the relative composition of non-refractory PM_1 plus BC and shows the contribution of different factors related to different sources retrieved from the OA fraction using PMF. In total, seven different factors were identified: OOA (oxygenated OA), SV-OOA (semi-volatile OOA), LV-OOA (low-volatile OOA), HOA (hydrocarbon-like OA), COA (cooking OA), BBOA (biomass burning OA) and CSOA (cigarette smoke OA, see Sect. 4.2.5; considered local contamination and not included in the pie charts in Fig. 2). Here, only a general overview of these different factors focusing on seasonal and spatial differences is given. A more detailed discussion of the various sources associated with these factors is provided in Sect. 4.2.

Meteorology overview:

The first period of the DIAPASON2013 campaign (23.-31.10.2013) was dominated by high pressure influences and low wind speeds with air masses moving from the Atlantic across Northern Africa and the Mediterranean basin. Within this period dust from the Sahara was transported to the Rome area (see Sect. 4.2.1). The second half of DIAPASON2013 (1.-7.11.2013) was characterized by a pressure drop and increased wind speed together with some frontal passages leading to precipitation. Both turbulent kinetic energy (TKE), which is a measure of the intensity of turbulence and can be used as an indicator for the mixing efficiency of pollutants in the air (Srivastava and Sarthi, 2002), and boundary layer heights (BLH) were at rather low levels during DIAPASON2013 (Table 3), favouring the accumulation of pollutants.

The first measurement days of POPE2013 (07.-09.11.2013) were influenced by changing weather conditions, followed by a low pressure system centred over Italy (10.-14.11.2013) driving N-NW wind conditions and leading to almost daily precipitation events. High TKE levels (almost three times higher compared to DIAPASON2013) and slightly increased boundary layer heights (900 m compared to 850 m; Table 3) led to conditions were dilution of pollutants was more favoured.

During DIAPASON2014 a low pressure system was located over the Atlantic and North Africa. ~~Saharan dust was advected to the measurement site during the first week of measurements. Some precipitation events occurred during these advections.~~Saharan dust was advected to the measurement site during the first week of measurements (Rizza et al., 2016). Some precipitation events occurred during these advections. TKE was slightly increased after the dust advection, favouring the reduction of pollutant concentrations. Boundary layer heights reached around 1500 m (Table 3).

During POPE2014 a period of low pressure over the Atlantic and high pressure over Africa and Europe (04.-13.6.2014) was followed by reversed conditions (14.-17.6.2014) with some heavy precipitation events. Compared to DIAPASON2014 the boundary layer was slightly higher (1560 m) and TKE was decreased by 20 %.

During DIAPASON2013 local winds were predominantly arriving from south and south-easterly directions, whereas during DIAPASON2014 south-westerly wind directions dominated (Fig. 1; no data available for POPE2013/2014, see Sect. 2.2). No clear relationships of air mass origin with measured PM_1 mass concentrations were found by the calculation of HYSPLIT (Stein et al., 2015) and FLEXPART (Stohl et al., 2005) backward trajectories for our measurement periods.

Aerosols and trace gases:

During both Oct/Nov and May/June measurements, CO_2, NO_x and particulate PAH concentrations (all typically traffic-related) were higher in central Rome compared to the outskirt location (Table 3). Cooking-related aerosol (COA) concentrations were found to be generally higher in the city centre (Fig. 2b, d), while traffic-related (HOA) concentrations were strongly increased during 2014 (+ 58 %) at the urban location (Fig. 2d), and nearly the same at both locations during the 2013 measurements (Fig. 2a, b). All this is consistent with increased primary emissions (cooking, traffic) at the urban (Fig. 2b, d) compared to the suburban site (Fig. 2a, c). However, total concentrations of organic aerosol predominantly of primary origin (POA) were higher at the suburban (1.9-2.5 µg m^{-3}) compared to the urban (1.4-1.6 µg m^{-3}) location. This is due to a factor indicating particles from biomass burning (BBOA), which was obtained exclusively at Tor Vergata (Fig. 2a, c). Here, biomass burning seems to be an important particle source, contributing the most abundant fraction (42-51 %) of POA. ~~Consistently,~~Note that due to the fact that OOA concentrations are significantly higher in the suburban site in 2013, the relative contribution of POA-related aerosol types (i.e. HOA, COA, and BBOA) is lower at the suburban location during this year. However, in order to avoid a bias in the comparison of the more locally generated POA-related aerosol types by advected aerosol mass, we compare the absolute mass concentrations for the different aerosol types at the different measurement locations/times. BC, which is related to primary emissions from both biomass burning and traffic, showed no general trend between the two locations (Table 3). Ratios of HOA/BC (DIAPASON2013: 0.26, POPE2013: 0.33, DIAPASON2014: 0.46, POPE2014: 0.53) were lower during fall 2013, indicating the more dominant contribution of biomass burning emissions to BC during this time. The fact that contributions from biomass burning to total BC concentrations are non-negligible was also found earlier (e.g. Crippa et al., 2013a). Generally, the HOA/BC ratios were higher in the urban compared to the suburban location in each year. This reflects the stronger influence of traffic emissions and the lower contribution of biomass burning emissions in the city centre.

The influence of increased temperatures and stronger solar radiation during measurements in May/June 2014 (Table 3) is reflected in elevated ozone mixing ratios and the fact that it was possible to extract an additional OOA factor, which was attributed to a fresher, less oxidised aerosol type (SV-OOA, Fig. 2c, d). This SV-OOA likely is the result of quick formation of secondary aerosol from precursors originating from the greater Rome area. Within a continuum of OOA with different degrees of aging/oxidation, SV-OOA (fresh, of rather local origin) and LV-OOA (aged, of more regional origin) are located in the upper and lower range, respectively. In contrast, during Oct/Nov, only one type of rather aged OOA was found (Fig. 2a, b), due to reduced photochemistry in this season which prevents the quick formation of oxygenated aerosol from precursors emitted in the vicinity.

A stronger influence of aged aerosol of rather regional origin on the PM_1 fraction was observed for May/June than for Oct/Nov: the fraction of OOA (SV-OOA + LV-OOA) to OA, but also the relative contribution of total organics and sulphate to PM_1 were higher in the warmer season (Fig. 2c, d). This could be caused by different prevalent air mass origins, though the analysis of backward trajectories provided no definite answers on this (see above). Also the relative fraction of sulphate could be ~~lowered~~lower in Oct/Nov due to an enhanced ~~fraction~~contribution of primary particles ~~as a consequence of lower boundary layer heights~~ (Table 3) as a consequence of lower boundary layer heights (which limits the dilution of locally produced aerosols while it does not influence the concentration of transported aerosols) and, potentially, higher emission strength of local sources during the colder season. Consistently, in Oct/Nov 2013 at both measurement locations a higher BC fraction was observed compared to May/June, and POA made up a larger fraction of the total measured organics (Fig. 2). Also absolute BC concentrations were enhanced. Additionally, higher concentrations of NO_x and PAH (increased by a factor of 3), and of total particle number concentration (PNC) were observed during Oct/Nov (Table 3), indicating the accumulation of pollutants during the colder season due to the aforementioned reasons.

"Home-made" vs. "advected" PM_1:

For a rough estimate of the contribution of PM_1 originating from sources in the Rome metropolitan area and from advection from outside, PM_1 species were separated into "home-made" (BC, HOA, COA, BBOA, SV-OOA, NO_3) and "advected" (OOA/LV-OOA, SO_4) (Table 4). NH_4 was apportioned to home-made and advected PM_1 based on the molar concentrations associated with NO_3 and SO_4, respectively. Not included in these estimates are dust advection periods and emissions from cigarettes (which were considered as local contaminations).While nitrate is formed quickly and thus strongly contributes to the "home-made" aerosol fraction, it can also be transported. The resulting fraction of "home-made" aerosol might therefore be slightly biased high, however by a few percent at most due to the small total contribution of nitrate to PM_1. For the POPE2013 measurements OOA shows only poor correlations with SO_4, but slightly better ones with NO_3, suggesting either a local contribution of OOA or the transport of NO_3. Whatever the case may be, it will contribute to the error of the estimation. During the measurements the fraction of home-made PM_1 accounted for 42-70 % and advected PM_1 accounted for 30-58 % of total (home-made + advected) PM_1 (Table 4). During the 2013 measurements higher absolute concentrations of home-made PM_1 were found at the suburban location compared to the urban site, possibly caused by meteorological conditions favouring pollutant accumulation during the respective period (see above). However, due to the large differences in total PM_1, the relative contribution of home-made PM_1 was higher at the urban location. During 2014, when meteorological conditions (e.g. BLH, TKE; see Table 3) were rather comparable at both locations, similar absolute concentrations of home-made PM_1 were observed at both sites. No general seasonal difference in home-made PM_1 fraction was observed, although BLH was strongly increased during the May/June 2014 compared to the Oct/Nov 2013 measurement periods. Partially, this might be due to the additional presence of the home-made species SV-OOA during May/June, which could to some extent have compensated for the dilution effect due to the increased BLH. Altogether, neither a general spatial (DIAPASON vs. POPE) nor a seasonal (Oct/Nov vs. May/June) tendency regarding the contribution of home-made and advected PM_1 to total PM_1 was observed. These results indicate that urban air quality in Rome strongly depends on both, emissions within the city and transport of pollutants to the city, which both contribute to urban aerosol concentration.

Independent of measurement season and location the organics fraction was always ~~was~~ found to contribute the largest share of PM_1 (44-53 % of non-refractory PM_1 plus BC, Fig. 2), though its relative composition (primary vs. secondary OA) differed. Regarding absolute PM_1 concentrations (Table 3 from EDM measurements, Fig. 2 from non-refractory components plus BC) neither any general conclusion whether aerosol mass concentrations are higher at the city centre or in the suburb, nor whether PM$_1$ concentrations are elevated during any of the two different seasons, can be drawn. In the 2013 campaign total PM$_1$ mass concentrations were more than doubled at the suburban compared to the urban location, whereas in the 2014 measurement PM$_1$ concentrations were increased by a factor of 1.4 at central Rome. As discussed above, changes in meteorological conditions are likely one explanation for this result: During DIAPASON2013 meteorological conditions favoured the accumulation of pollutants, whereas the dilution of pollutants was favoured during the POPE2013 measurement period; during DIAPASON2014 and POPE2014 TKE and BLH were rather similar leading to comparable pollutant dilution effects during the two measurement periods. BLH were increased by around 75 % during May/June compared to Oct/Nov 2013, leading to stronger dilution capacities in general. In addition to meteorological conditions (e.g. solar radiation, BLH, TKE, air mass origin, etc.) local air quality can be strongly influenced by local emission from various sources (traffic, cooking, biomass burning). A strong influence of meteorological conditions (air mass origin) on air quality was also observed during the MEGAPOLI campaign in Paris in July 2009, where variations in secondary aerosol concentration mainly were attributed to such reasons (Freutel et al., 2013).

4.2 Aerosol sources: identification and characterisation

In this section the various aerosol types and sources which were identified from the data obtained during the DIAPASON and POPE measurement campaigns in 2013 and 2014 are discussed in more detail. Each identified aerosol type was characterized in an attempt to determine its contribution to total particulate mass and its seasonal and spatial variability. Furthermore, the potential origin of the identified aerosol types is discussed.

4.2.1 Saharan dust

During each DIAPASON field campaign one dust advection event lasting for several days was observed. The identification of the dust events with dust reaching down to the ground was based on dust forecasts provided by the SKIRON model (Kallos et al., 1997) and on co-located polarisation LIDAR-ceilometer measurements (~~Gian Paolo Gobbi, personal communication). PIXE analysis of 1-hour filter samples confirmed a significant increase of mineral dust concentrations at ground level during the identified dust periods (Silvia Nava, personal communication 2016).~~data can be found at www.diapason-life.eu). PIXE analysis of

1-hour filter samples confirmed a significant increase of mineral dust concentrations (i.e. Na, Mg, Si, Al, Ti, K, Ca, Fe; Nava et al., 2012) at ground level during the identified dust periods (Barnaba et al., in preparation 2016). Table 5 provides the time intervals of "dust" and "no dust" (i.e. background with respect to dust advections) periods for DIAPASON2013 and DIAPASON2014. Based on these, estimations regarding the contribution of dust to PM levels were made by calculating the coarse particle fraction ($PM_{10-2.5}$) from EDM measurements for the respective periods (Table 5).

During DIAPASON2013 a Saharan dust advection period was observed from the beginning of the measurements (October ~~29th (5 pm~~23th) until November 1st ~~(8 am)~~ with $PM_{10-2.5}$ concentrations at ground level being increased by ~~78~~80 % with respect to background conditions. Total PM_{10} concentrations were elevated by ~~68~~150 %, with ~~68~~71 % and ~~70~~57 % of mass belonging to PM_1 during the ~~background~~dust event and during the ~~dust event~~background periods, respectively. This increase in absolute PM_1 with ~~a slight~~an increase in the fraction of PM_1 during the dust advection compared to background conditions was also reflected in the particle size distributions (Fig. 3, black traces). The dust event was also forecasted by the BSC-DREAM8b model (Basart et al., 2012; Perez et al., 2006a; Perez et al., 2006b) and also HYSPLIT (Stein et al., 2015) back trajectories showed dust transport from the Sahara with main dust sources located at 30-33N, between Morocco (Saharan Atlas) and SW Tunisia (Erg Oriental), in the period 26.-28.10.2013, moving along an anti-cyclonic pattern.

During DIAPASON2014 a dust event was observed from May 20th (1 pm) until May 26th (9 am). Here, the coarse particle fraction ($PM_{10-2.5}$) was increased by 180 % compared to the "no dust" interval with much smaller fractions of particle mass in PM_1 (31 and 48 % in the "dust" and "no dust" periods, respectively). The contribution of dust to the coarse particle fraction with almost no contribution to the submicron fraction is reflected in the difference particle mass size distribution (Fig. 3, bottom panel, red trace), which shows maximum mass concentrations for aerodynamic particle diameters around 2 µm and smaller contributions extending down to ~600 nm and up to more than 10 µm particle diameter. Comparing both dust events in terms of particle sizes, the contribution of the dust advection event during DIAPASON2014 was characterized by a broad particle mass size distribution with maximum concentrations at particle sizes around 2 µm, whereas in 2013 two modes (with maxima around 0.6 µm and 3 µm) were observed. Both the BSC-DREAM8b model and HYSPLIT back trajectories showed dust transport from the Sahara to occur between 19.-22.05.2014 along a cyclonic pattern, with dust originating (as in October 2013) at 30-35N between Morocco (Saharan Atlas) and SW Tunisia (Erg Oriental).

With regard to the coarse particle mode (PM$_{10-2.5}$) the dust event during DIAPASON2014 was more distinct. In terms of absolute PM$_{10}$ concentrations, higher concentrations at ground level were reached during the dust advection measured during DIAPASON2013. However, with respect to the "no dust" conditions, mean ~~contributions~~PM$_{10}$ increases of ~~approximately 10~~about 17 and 11 µg m^{-3} ~~dust to PM$_{10}$ concentrations~~ were observed during DIAPASON2013 and DIAPASON2014, respectively. This agrees well with the ~~campaigns in both years, which is lower than the mean increase of PM$_{10}$~~ observations made by Gobbi et al. (2013), who reported PM$_{10}$ concentrations in the order of 12-16 µg m^{-3} ~~observed by Gobbi et al. (2013)~~ during dust advection events in the period 2001-2004. During both advection events legal PM$_{10}$ limits of the European Union (daily mean value of 50 µg m^{-3}) were not exceeded.

AMS data were investigated for potential impacts of Saharan dust advections on the chemical composition of non-refractory submicron particles. Figure 4 presents the mean chemical composition of non-refractory PM$_1$ measured during "dust" and "no dust" periods for both DIAPASON campaigns. Only in 2013 ~~minor~~ differences in absolute mass concentrations were observed, consistent with ~~the slight increase of~~higher submicron ~~particles~~particle concentrations observed in the mass size distributions during this dust event (Fig. 3, bottom panel, black trace). This difference in PM$_1$ concentration between the dust and no dust period is likely due to differences in air mass origin. Whereas during the dust period air masses preferentially arrive from the Mediterranean region, the no dust period is mainly influenced by air masses from the Atlantic Ocean. However, the relative composition remains nearly the same for both periods in both years. This result suggests that there was no significant influence of the dust advection on the chemical composition of the submicron non-refractory aerosol fraction.

In order to cross-check whether differences in meteorological conditions could have biased these results, and e.g. could have compensated for changes due to the dust affecting non-refractory PM$_1$, averages of meteorological variables were calculated for "dust" and "no dust" periods. The only slight differences found between dust events and background conditions were in local wind directions (SE compared to S~~/SE~~ in 2013, and SW compared to SSW in 2014) and (in 2013) in wind speeds ((1.~~4~~5 ± 0.~~7~~8) m s^{-1} compared to (2.~~0~~7 ± 1.6) m s^{-1}). Since these differences are only very minor, we conclude that our observation of comparable chemical composition of non-refractory PM_1 during “dust” and “no dust” periods was not caused by any compensating effects.

4.2.2 Secondary and aged aerosol: seasonal influence on formation processes and chemical composition

Seasonal variations of the characteristics of secondary and aged aerosols were identified by investigating new particle formation events and particle chemical composition measured during both POPE and DIAPASON campaigns in Oct/Nov 2013 and May/June 2014.

New particle formation:

Diurnal cycles of size-resolved and total particle number concentrations (PNC) for the Oct/Nov 2013 and May/June 2014 campaigns (Fig. 5) revealed several seasonal differences. During measurements in Oct/Nov 2013 (Fig. 5, left panels), elevated PNC were only observed during rush hour times in the morning and the evening, whereas in the measurements in May/June 2014, an additional PNC peak occurred with a maximum around 1-3 pm (DIAPASON2014) and 2-3 pm (POPE2014), respectively (Fig. 5, right panels). At the urban site (Fig. 5, bottom panels), PNC after the morning rush hour remain at an elevated level, likely because of increased background concentrations due to generally higher traffic density in the city centre. PNC were generally higher in the Oct/Nov 2013 than in the May/June 2014 campaigns, as discussed in Sect. 4.1.

Mean particle number size distributions for the period of maximum PNC at midday (Fig. 6; “nucleation”; solid traces) show a distinct mode at small particle diameters between 7-15 nm for both May/June 2014 campaigns (also visible in Fig. 5, right panels) compared to the number size distribution measured between 10-11 am (Fig. 6; “background”; dashed traces). Such occurrences of ultrafine particles at midday, when concentrations of particles from traffic are at a relative minimum and thus not responsible for strongly increased PNC, have been attributed before to new particle formation characteristic for urban areas with high solar radiation (Brines et al., 2015; Minguillon et al., 2015; Reche et al., 2011). During POPE2014 an additional mode at larger particle sizes (D_p approximately 15-50 nm) was found in the particle size distribution measured at midday (Fig. 6), probably originating from increased background levels.

During POPE2014 diurnal cycles of mean (grey) and median (black) PNC agree very well with each other, also during the midday peak (Fig. 5). This reflects the observed low day-to-day variability during this period for the measurements in central Rome, wherein the corresponding PNC time series a midday peak was observed on every single day. Local smoking activities (see Sect. 4.2.5) at the central Rome measurement location seem not to have biased these results, since no differences in diurnal cycles of PNC for weekdays (smoking activities) and weekends (no smoking activities) have been found. This suggests that the formation of new particles around midday was taking place every day at central Rome during the May/June 2014 measurement period.

Conversely, the diurnal cycle of total PNC measured during DIAPASON2014 shows a clear discrepancy between mean and median values during the midday peak (Fig. 5). This discrepancy is due to the fact that new particle formation events did not occur on all days, probably induced by different meteorological conditions and/or differences in pre-existing particle surface areas (e.g. Kulmala and Kerminen, 2008).

To test whether particular meteorological conditions can promote/suppress new particle formation events, “nucleation” and “non-nucleation” days were classified for DIAPASON2014 by comparing PNC measured during 10-11 am (background conditions, PNC_{bg}) and during 11 am - 4 pm (typical nucleation periods, PNC_{nuc}) (Table 6). This classification was cross-checked by verifying if during classified nucleation days a clear increase in PNC at small particle diameters ($D_p \leq 25$ nm) could be observed in the particle number size distributions, and whether it was missing on classified non-nucleation days. Only one potentially falsely classified nucleation day (24.05.2014) was found by checking these criteria, and was moved to the class of non-defined days. The classification resulted in six nucleation days, six non-defined days and two non-nucleation days.

Mean values for the time period 10 am to 4 pm (new particle formation period plus one previous hour) were calculated for each day and averaged according to the above-mentioned classification for the DIAPASON2014 campaign. Table 6 lists PNC of the classified periods and variables potentially supporting new particle formation. A slight trend of increased temperature, solar radiation and ozone levels and of low relative humidity characterizes nucleation days compared to non-nucleation days and non-defined days. This is consistent with previously reported association of high solar radiation (Pikridas et al., 2015; Shi et al., 2001), low relative humidity (Kulmala and Kerminen, 2008) and increased ozone concentrations (Harrison et al., 2000) with new particle formation events. No relationship between the occurrence of new particle formation and the presence of Saharan dust was observed. Different to the findings of Zhang et al. (2004), no increase of sulphate, ammonium and nitrate concentrations was observed in our measurements during periods with new particle formation events. Estimations based on the size distribution measurements during DIAPASON2014 reveal that less than 1 % of PM_1 can be assigned to particles generated by new particle formation. Therefore, it is not surprising that no significant influence of the particle formation events on the AMS-measured chemical particle composition could be observed.

In summary, our data do not provide sufficient statistical evidence to unequivocally determine the driving factors for new particle formation. However, since indications for such were only observed in the warmer season at both locations, it is probably linked to higher temperatures and stronger solar radiation. Similar results were obtained from the MEGAPOLI measurements in Paris, where new particle formation was only observed during summer (Pikridas et al., 2015). During the May/June 2014 campaigns, new particle formation events occurred roughly on 43 % of the measurement days at the suburban location, but on each single day at central Rome, potentially due to increased concentrations of precursors and higher prevailing mean temperatures (Table 3). In a long-term measurement study performed by Costabile et al. (2010) the occurrence of aged nucleation mode particles (up to 30 nm) was observed predominantly in spring in the area of Rome at a regional background site (located more remotely than the Tor Vergata site) in the early afternoon (3 pm) when the measurement site was located downwind of Rome (Brines et al., 2015). In contrast, during DIAPASON2014 measurements, no dependency between nucleation events and wind direction was observed, and the site was not located downwind of Rome during nucleation periods. At this measurement location, probably ~~less~~lower concentrations of precursors are available than in central Rome, but ~~more precursors~~higher concentrations than at a remote regional background site such as in the study of Costabile et al. (2010). This probably facilitates new particle formation events in the direct vicinity of the site under favourable meteorological conditions, but independent of advection of air masses from central Rome.

Secondary and aged aerosol:

Because of extremely low mass contributions from freshly formed particles to total particle mass, new particle formation had no influence on the measured total organics mass concentrations. However, a general seasonal difference in the composition of the oxygenated organic aerosol (OOA) as determined in the PMF analysis was found, as discussed in the following.

OOA, an aerosol type with increased oxygenation level, typically dominates the OA fraction. It is assumed to be mainly formed in the atmosphere from gaseous biogenic and anthropogenic precursors by photochemical oxidation, thus indicating SOA. Additionally, some OOA may originate from atmospheric aging of POA. Generally, aging processes are reflected in an increased degree of aerosol oxidation (Jimenez et al., 2009) leading to a larger fraction of *m/z* 44 (CO_2^+) in the aerosol mass spectra, generated by thermal decomposition of carboxylic acids in the AMS ~~(Ng et al., 2010).~~(Alfarra et al., 2004). Additionally, a prominent peak in OOA mass spectra occurs at *m/z* 43 ($C_3H_7^+$ and $C_2H_3O^+$). Under conditions where sufficient freshly oxidised organic aerosol is available in the ambient air, PMF can separate the OOA into two factors~~ associated with mass spectra containing different relative fractions of *m/z* 44 and *m/z* 43 (f44 and f43, ratio of *m/z* 44 and *m/z* 43 signal, respectively, to the total signal of organics): (I) A less oxidised, fresher, more locally produced semi-volatile OA (SV-OOA) associated with higher f43, and (II) a stronger oxidised, more aged low-volatile OA (LV-OOA) associated with higher f44 (Ng et al., 2010).~~. These factors differ in their relative fractions of *m/z* 44 and *m/z* 43 (f44 and f43, ratio of *m/z* 44 and *m/z* 43 signal, respectively, to the total signal of organics), which reflects their different degrees of oxidation. The factor associated with higher f43 indicates a less oxidised, fresher, more locally produced semi-volatile OA (SV-OOA), whereas a higher f44 indicates a stronger oxidised, more aged low-volatile OA (LV-OOA) (Ng et al., 2010).

During our measurements the relative contribution of OOA to total organics varied between 42-76 %, with a slight increase during the warm period (Fig. 2). However, the main seasonal difference was found in the composition of the OOA fraction. During the Oct/Nov 2013 campaign only one type of OOA was found, whereas for May/June 2014 PMF analysis resulted in two OOA-factors: SV-OOA and LV-OOA. This ~~observation~~ is ~~typical for~~ typically only observed during summer conditions~~ with higher temperatures~~, when the dynamic range of temperature, ozone concentration and ~~stronger~~ solar radiation~~, associated with increased photochemistry~~ is large, which is assumed to be the main driving force for the variability of the OOA volatilities (Jimenez et al., 2009)~~, which enhance secondary aerosol formation and aging processes and therefore facilitate the separation of OOA into fractions of different aging levels.~~. Similar observations were made during the MEGAPOLI measurements in Paris, where only one factor describing OOA was identified in winter (Crippa et al., 2013a), whereas during summer SV-OOA and LV-OOA could be separated (Crippa et al., 2013b).

The ratio of f44 to f43 gives an indication on the mean aging level of the aerosol (Fig. 7; Ng et al., 2010). LV-OOA (from DIAPASON and POPE 2014, red markers) and OOA (from DIAPASON and POPE 2013, green markers) fall into the same region in the f44 vs. f43 plot (Fig. 7), indicating similar aging stages. SV-OOA (from DIAPASON and POPE 2014, blue markers) shows a much higher fraction of *m/z* 43 together with a decreased *m/z* 44 fraction, which suggests a low-oxidised, less aged particle type. Also the recombined “LV-OOA+SV-OOA” (black markers in Fig. 7) shows a stronger contribution of f43 compared to OOA, indicating an overall higher fraction of less oxidised organic aerosol in the warmer season. We assume that LV-OOA (and OOA) is mainly advected and consists of strongly processed material, whereas the low oxidation level of SV-OOA suggests a fresh, more locally produced aerosol which was quickly formed from regional precursors as a consequence of increased photochemistry during this season.

This hypothesis is tested by the use of polar plots, which connect species concentration with information on local wind direction and speed, thereby indicating the origin of a certain type of aerosol (see Sect. 3.1). Figure 8a shows the colour coded concentration of SV-OOA, LV-OOA, NH_4, NO_3 and SO_4 depending on wind direction and speed obtained during the DIAPASON2014 measurements. SV-OOA concentrations are increased during low wind speed conditions, indicating nearby, no-buoyance sources. In contrast, LV-OOA concentrations are almost independent of wind speed with only slightly increased concentrations during periods of high wind speed with mainly south-westerly wind directions (direction of Tyrrhenian Sea). This suggests that LV-OOA is not associated with sources located in the vicinity of the measurement site, but long-range transported to the site e.g. over the ocean or from central Europe. The polar plot characteristics of NO_3, which is often used as a tracer for semi-volatile aerosol (DeCarlo et al., 2010; Lanz et al., 2007), show strong similarities to the ones of SV-OOA (Fig. 8a). Also SO_4 and LV-OOA show polar plot patterns similar to each other (Fig. 8a), confirming the characteristics of an aged, regionally transported aerosol. The polar plot of NH_4 shows a hot spot at low wind speeds in northern direction, which is also reflected in the patterns of SV-OOA and NO_3. Increased NH_4 concentrations are also observed at higher wind speeds in south-westerly direction, agreeing with the polar plot patterns of LV-OOA and SO_4.

The polar plot of OOA obtained for DIAPASON2013 shows increased concentrations particularly during periods of north-easterly, but also during south-westerly wind directions (Fig. 8b). During conditions of low wind speed, OOA concentrations are increased independent of the prevailing wind direction. In contrast to the findings for DIAPASON2014, for this data set similar polar plot characteristics as for OOA were observed partly in the plots of NO_3, NH_4 and SO_4 (Fig. 8b). Elevated NH_4 and SO_4 concentrations were mainly measured during times with south-westerly wind direction, whereas for NO_3 ~~was~~ rather ~~advected from~~an increase for north-easterly ~~direction.~~directions was observed. Based on the polar plot characteristics no consistent trend indicating the degree of aging~~ level~~, the source or the formation process of the OOA fraction can be observed, consistent with the assumption of advection of a rather aged type of OOA together with different amounts of NO_3, SO_4 and NH_4 depending on air mass history.

4.2.3 Particles from biomass burning

The type of primary organic aerosol at Tor Vergata identified from PMF analysis which had the largest share during both measurement periods was attributed to biomass burning (biomass burning OA, BBOA). BBOA was identified by comparison with the time series of known ion fragments of levoglucosan ($C_3H_5O_2^+$ (*m/z* 73) and $C_2H_4O_2^+$ (*m/z* 60); Schneider et al., 2006) and by correlating the BBOA mass spectra with those presented by Mohr et al. (2012). With Pearson's R^2 = 0.57-0.59 rather poor correlations were obtained, which demonstrates the complexity and the potential variations of the BBOA mass spectra due to aging processes and differences in source processes (e.g. different burning conditions or fuels; Weimer et al., 2008). The mean BBOA mass concentration was 1.28 µg m^{-3} (24 % of total OA) during Oct/Nov 2013 and 0.82 µg m^{-3} (18 % of total OA) during May/June 2014, respectively (Fig. 2). Increased BBOA concentrations during the colder season probably result from stronger agricultural burning activities (green waste burning) and potentially domestic heating, as well as from lower boundary layer heights. However, due to the moderate temperatures also during the Oct/Nov 2013 measurements, we do not expect strong contributions from domestic heating. In the evening of 25.10.2013 during a strong, visually detectable biomass burning event, which could be related to green waste burning in the nearby Alban Hills, maximum concentrations of BBOA were obtained (up to 75 µg m^{-3}). This event was used during the identification of the PMF solution~~: Only~~, since only a factor including this event could be considered to be attributed to biomass burning emissions.

The origin of BBOA emissions was further investigated by relating BBOA mass concentrations to local wind direction and speed (see Sect. 3.1). The resulting polar plots (Fig. 9) indicate BBOA particles mainly arriving from south-easterly directions during DIAPASON2013. During this measurement period agricultural fires were frequently observed in the Alban Hills (Frascati vineyard area), which are located in this direction. Additionally, BBOA was observed during conditions of north-easterly winds and higher wind speeds (up to 4 m s^{-1}), possibly resulting from residential wood burning in a densely populated urban periphery area (Borghesiana). The polar plot of BBOA obtained from DIAPASON2014 measurements does hardly point to any preferential direction of BBOA origin. Since elevated BBOA concentrations were mainly reached during low wind speed conditions, emission from rather local sources is suggested.

BBOA was not identified in the measurements in the city centre of Rome, even not in PMF solutions with a large number of factors (8). Since green-waste burning and domestic heating with biomass are forbidden in central Rome, biomass burning related particles are probably not emitted in the local environment. However, the contribution of biomass burning and domestic heating to the urban air pollution of Rome (especially during winter time) was reported by Gariazzo et al. (2016). Apparently, during our measurements in late spring and autumn the contribution of particles emitted outside the suburban area is too small to be identified with PMF and/or aging processes during the transport of the particles lead to a loss of the BBOA fingerprint (Bougiatioti et al., 2014). Also during the MEGAPOLI measurements in Paris emissions from biomass burning were identified in the organic aerosol fraction (Crippa et al., 2013a). In contrast to our measurements, in Paris BBOA was only found during the winter time campaign (Jan/Feb), but also at the measurement location in the city centre, probably generated by local domestic wood burning (Crippa et al., 2013a).

In summary, the results from both DIAPASON measurements show that particles from biomass burning significantly (18–24 % of total OA) contributed to local air pollution in the suburban area in late autumn as well as in late spring. Agricultural fires and possibly wild fires probably are their most important sources, since heating activities are assumed to be quite low at these times due to the moderate temperature conditions (Table 3).

4.2.4 Emissions related to traffic and cooking activities

At both measurement locations, during both seasons particles from traffic- as well as from cooking-related emissions were detected.

Indications of traffic-related emissions can be found in several measured variables showing a distinct diurnal pattern with peaks during the morning and evening rush hours. The time series and diurnal pattern of HOA (hydrocarbon-like organic aerosol), a PMF factor that is typically associated with traffic emissions, show good agreement with the respective patterns of species like BC, NO_x and PAH (diurnal cycles: $R^2 > 0.85$) for all four campaigns. Also correlations of complete campaign time series of HOA with BC result in good agreements ($R^2 \approx 0.7$).

In the diurnal cycles of HOA seasonal and spatial differences can be observed (Fig. 10). Independent of season and measurement location a short peak occurs during the morning rush hour and a broader peak starting during the evening rush hour. During all field campaigns except DIAPASON2013, HOA concentrations remain increased throughout the night. Thus, the exact period of the evening rush hour cannot be clearly isolated. These differences in the shapes of the HOA peaks in the morning and evening rush hour are mainly controlled by boundary layer dynamics together with the diurnal cycle of traffic-related emissions (rush hour times). A seasonal difference is observed in the HOA evening rush hour peak, which peaks around midnight during May/June, but around 7-8 pm during Oct/Nov. This shift and the broadening of the HOA peak in May/June 2014 is probably driven by the different boundary layer dynamics during the two seasons.

For both measurement years a time shift of the morning peak between Tor Vergata and central Rome (later by about one hour) can be observed. Since similar diurnal temperature profiles measured at the suburban and the urban location suggest also similar boundary layer dynamics at the two sites, the observed shift possibly results because traffic starts in the suburbs earlier in the morning and continues slowly towards the city centre. In contrast to our observations, from BC measurements during the MEGAPOLI summer campaign in Paris no distinct shift of the morning rush hour peak was observed between the two suburban and the urban measurement locations (Freutel et al., 2013).

Mean HOA mass concentrations for the individual measurement campaigns range between 0.59-0.93 $\mu g\ m^{-3}$. During the 2013 measurements (Oct/Nov) similar concentrations were obtained at the suburban site ($0.76 \pm 1.04\ \mu g\ m^{-3}$) and central Rome ($0.71 \pm 0.72\ \mu g\ m^{-3}$), whereas in 2014 higher concentrations were reached at central Rome ($0.93 \pm 0.73\ \mu g\ m^{-3}$)

compared to the suburb (0.59 ± 0.60 µg m^{-3}). Overall, the contribution of traffic-related emissions (e.g. HOA, NO_x, PAH) to local air pollutant levels was higher in central Rome, as already discussed in Sect. 4.1.

A factor associated with cooking emissions, COA (cooking OA), was obtained by PMF analysis of the OA measured at both locations and during both seasons. The COA mass spectra show prominent peaks at *m/z* 41 and 55 (Allan et al., 2010; Lanz et al., 2007) and a smaller contribution of *m/z* 60 and 73 (Mohr et al., 2009). Our COA mass spectra correlated well with those found by Faber et al. (2013) and Mohr et al. (2012) with R^2 = 0.63-0.93.

The COA diurnal cycles observed at central Rome (Fig. 11, upper panel) are consistent with results from previous studies (e.g. Allan et al., 2010; Mohr et al., 2012) showing highest concentrations in the late evening (around 10 pm) and a smaller peak around midday (2-3 pm). This pattern is generated by a combination of source strengths and boundary layer dynamics, with typically increased boundary layer height during lunch time compared to dinner time.

In contrast, diurnal cycles of the COA factors measured at the suburban location in 2013 and 2014 (Fig. 11, lower panel) both show a peak in the evening, but only during DIAPASON2014 a slight and barely significant COA concentration increase was observed during lunch time. This could be due to an insufficient separation of the COA and HOA factor during PMF analysis, which is also demonstrated in the COA “morning peak” of the DIAPASON2014 measurements. However, the missing midday peak also reflects the generally low abundance of cooking-related OA at the suburban measurement location: while there are strong cooking activities and a large abundance and closeness of restaurants around the central Rome site, potential sources in the immediate vicinity of the suburban site are scarce. At a distance of around 250 m from our monitoring site, a cafeteria served hot meals for lunch, but apparently, our measurements were not strongly affected by its emissions.

Consistently, absolute mass concentrations of cooking-related emissions were higher at the central Rome site (0.70 ± 1.00 µg m^{-3}, 0.65 ± 0.69 µg m^{-3} in 2013 and 2014, respectively) compared to the suburban measurement location (0.45 ± 0.50 µg m^{-3}, 0.53 ± 1.29 µg m^{-3}). Ranging between 8-29 % of the total OA concentrations, cooking activities contribute significantly to (sub-) urban air pollution. During meal times the contribution of COA to total organics can be very high~~:~~. For example during lunch/dinner times at central Rome, COA contribution to total organics was 35 %/53 % (POPE2013) and 9 %/25 % (POPE2014), respectively. Similar observations were made during the MEGAPOLI winter measurements in Paris, where COA contributed on average 11-17 % to total OA (up to 35 % during lunch times) (Crippa et al., 2013a).

4.2.5 Cigarette smoking emissions

For both POPE campaigns in central Rome PMF analysis of the organic aerosol fraction resulted in a factor which could be associated with cigarette smoke (CSOA; excluded from Fig. 2). This was not very surprising, since cigarette smoking took place in the direct vicinity of the measurement location. The mass spectra of CSOA from both years show good correlation with each other ($R^2 = 0.7$; Fig. 12). Very characteristic for the CSOA spectra is a peak at *m/z* 84 from $C_5H_{10}N^+$ and a peak at *m/z* 42 resulting from the ion $C_2H_4N^+$ (Fig. 12). ~~This ion (*N*-methylpyrrolidine) is~~Both ions are typically observed in EI mass spectra of nicotine (NIST: http://webbook.nist.gov, last access ~~09~~11.~~05~~11.2016~~) and~~). $C_5H_{10}N^+$ (*N*-methylpyrrolidine), which shows the strongest signal in the EI mass spectrum of nicotine, is generated by cleavage of the nicotine molecule into two heterocycles (Jacob III and Byrd, 1999). Since nicotine is one of the most abundant particulate compounds identified in cigarette smoke samples (Rogge et al., 1994), its fragments are suitable tracers for cigarette emissions. While cigarette smoke-related aerosol has been found in AMS measurements previously (Faber et al., 2013; Fröhlich et al., 2015) and also the detection of nicotine from cigarette smoke was mentioned (Jayne et al., 2000), to our knowledge, the identification of the nicotine fragment *N*-methylpyrrolidine from analysis of HR-ToF-AMS data is reported here for the first time. The time series of $C_5H_{10}N^+$ was used during the evaluation of the PMF results as tracer for CSOA, yielding good correlations ($R^2 > 0.9$) with the time series of CSOA. The correlation of the time series of $C_2H_4N^+$ with CSOA is slightly poorer ($0.83 < R^2 < 0.9$). Since also the difference of the contribution of the ion $C_2H_4N^+$ to the mass spectra of CSOA compared to the mass spectra of other factors is less pronounced than for the ion $C_5H_{10}N^+$ the latter one seems to be more specific for cigarette emissions than $C_2H_4N^+$. This is why the use of $C_5H_{10}N^+$ as a tracer ion for cigarette emissions was favoured over the ion $C_2H_4N^+$.

The CSOA mass spectra from both POPE campaigns show reasonable to very good agreement with CSOA mass spectra reported by Faber et al. (2013) ($0.65<R^2<0.96$). Some differences are observed between the mass spectra obtained for POPE2013 and 2014 in the relative fraction of CO_2^+ and its related ions, which also affects the observed elemental ratios

(Fig. 12). This results in a potential error in CSOA concentrations of less than 10 % and probably is due to a PMF artefact and/or insufficient correction for gas phase CO_2. Comparison with mass spectra of cigarette smoke obtained in the laboratory (Faber et al., 2013) show a contribution of CO_2^+ more similar to the POPE2013 measurements. Further laboratory work in order to obtain more robust source spectra is needed to better constrain the expected f44 in CSOA mass spectra. Due to the low intensity of the N-containing ions and a conservative selection of ions which were fitted in the mass spectra reported by Faber et al. (2013), the nicotine fragment ($C_5H_{10}N^+$) was not observed in their measurements of cigarette smoke. However, after re-analysis of the mass spectra with integration of the $C_5H_{10}N^+$ ion in the fitting procedure, a contribution of the nicotine tracer ion is clearly visible (Peter Faber, personal communication).

Also the time series of mass concentration of the CSOA factor clearly support its attribution to cigarette smoking emissions. The diurnal cycle of the CSOA factor strongly correlates with typical working hours at the measurement location and with the diurnal cycle of the marker fragment $C_5H_{10}N^+$ (R^2 = 0.98 for POPE2013 and POPE2014), exemplarily shown for POPE2014 in Fig. 13 (top). Averaged CSOA mass concentrations for each day of the week (Fig. 13; bottom) show distinct differences between working days and weekend, when the administration of the hospital where the measurements took place was closed, supporting the attribution of this PMF factor to locally emitted CSOA. Very similar observations were made during the POPE2013 measurements.

Particles from cigarette smoke contributed 9-24 % (0.62-0.76 µg m^{-3}) to the total organic aerosol mass measured at the location in central Rome. No indications for cigarette emissions were found during the DIAPASON measurements. This result shows a potentially strong influence on air quality in the direct environment of smokers, like it was also observed by Faber et al. (2013) and Fröhlich et al. (2015). Since in our measurement, CSOA is mostly produced close to the measurement location (i.e. can be regarded a local contamination), it was not included in the previous analyses of organic aerosol composition (see Sect 4.1).

$C_5H_{10}N^+$ as a potential CSOA marker ion: The ion $C_5H_{10}N^+$ was further investigated in order to assess its applicability and limitations as a tracer for cigarette emissions in AMS data sets. While the nicotine fragment ion $C_5H_{10}N^+$ (*m/z* 84.08) seems to be unique to cigarette emissions, the proximity of the ions $C_5H_8O^+$ (*m/z* 84.06) and $C_6H_{12}^+$ (*m/z* 84.09) in the mass spectra causes interferences, since the mass resolution of the instrument (R ≈ 2000 in V-mode) is not sufficient for completely separating the individual ion signals. Mass spectra of

the primary organic aerosol PMF factors (HOA, COA, BBOA) which are not related to cigarette emissions ("POA_{noCSOA}") show significant contributions (0.2 to 0.7 % of total organics mass spectral signal) of the ions $C_5H_8O^+$ and $C_6H_{12}^+$, leading to an artificial increase of the nicotine tracer ion signal. In contrast, for OOA mass spectra the contribution of these ions is comparatively low (0.1 % of total organics mass spectral signal), which is why a potential interference of OOA was neglected in the following considerations.

AMS measurements performed during DIAPASON2013 and DIAPASON2014, which are assumed to be not influenced by local cigarette emissions, were used to quantify the concentration-dependent influence of POA_{noCSOA} on the nicotine tracer ion $C_5H_{10}N^+$ due to fitting interferences from the neighbour ions $C_5H_8O^+$ and $C_6H_{12}^+$. A linear relationship between $C_5H_{10}N^+$ and POA_{noCSOA} was observed for a POA_{noCSOA} concentration range of 0-10 µg m^{-3}. Using the mass contribution of $C_5H_{10}N^+$ to the total CSOA mass spectra (Fig. 12; 1.8 % and 1.9 % for POPE2013/2014, respectively), the corresponding ion signals were converted into CSOA detection limits. It was found that, under conservative considerations, CSOA concentrations of at least 10 % of POA_{noCSOA} are needed in order to exceed detection limits. During conditions of negligible POA_{noCSOA} concentrations, a CSOA detection limit of 80 ng m^{-3} was estimated.

The same considerations were performed for the ion $C_2H_4N^+$ in order to evaluate its applicability as a nicotine tracer. In contrast to $C_5H_{10}N^+$, the ion $C_2H_4N^+$ seems to be less affected by its neighbouring ions. Therefore we assume that its occurrence in the mass spectra of different PMF factors does not only result from interferences of signals, but that $C_2H_4N^+$ is also included in non-CSOA factors. However, the contribution of $C_2H_4N^+$ to the CSOA mass spectra is higher than its contribution to those of other aerosol species (1-2 % instead of 0.1-0.6 %). Therefore, we would recommend using $C_2H_4N^+$ as a second nicotine tracer, but only in combination with $C_5H_{10}N^+$.

Based on these estimations, it can be concluded that $C_5H_{10}N^+$ is a suitable nicotine tracer ion for HR-AMS measurements which are influenced by local cigarette emissions (i.e. CSOA larger than 10 % of POA_{noCSOA}) and can be used to estimate CSOA concentrations or to identify a CSOA factor from PMF analysis. Urban background concentrations of cigarette-related particles in the range of 1 % of PM_1, as reported by Rogge et al. (1994), however, are below the estimated CSOA detection limits. This is still true when considering typical contributions of OOA to total organics (~50 %) and of OA to PM_1 (also ~50 %), leading to a CSOA detection limit of around 2.5 % of PM_1. In order to identify cigarette smoke contributions in the order of 1 % of PM_1, higher mass spectral resolution is needed to be able to separate the nicotine tracer ion from its neighbouring ions. Nevertheless, the fitting of $C_5H_{10}N^+$ at *m/z* 84 and also $C_2H_4N^+$ at *m/z* 42 could be worthwhile for HR-AMS data sets which are potentially influenced by cigarette-related particles. In future work, it should be investigated how aging processes affect the appearance of ~~this~~the marker ion $C_5H_{10}N^+$ in the mass spectra.

5 Summary and conclusions

Intensive field campaigns have been performed during Oct/Nov 2013 and May/June 2014, each time consecutively at two locations (suburban, urban) in the area of Rome, enabling the study of seasonal and spatial differences of aerosol and trace gas characteristics.

During both years at the suburban location an impact of advected Saharan dust on PM_{10} levels was detected. With respect to background conditions, increases of PM_{10} by ~~68~~150 % (2013) and 100 % (2014) were measured, corresponding to average absolute increases of about ~~10~~12-17 µg m^{-3}. No influence of the dust occurrence on the non-refractory PM_1 chemical composition was found during the advections.

At both locations, during the Oct/Nov measurements air quality was more strongly influenced by primary emissions (e.g. BC, NO_x, PAH) with generally increased particle number concentration (PNC), whereas during May/June the contribution from secondary particles (sulphate, aged OA) and ozone was more important. Also during May/June 2014, new particle formation was frequently detected around midday, while in the colder season no distinct increase of PNC took place outside typical rush hour times. The consequence of higher temperatures plus stronger solar radiation was also visible in the SOA-related fraction of the organic aerosol: During the warmer season two types of OOA (less oxidised, fresher SV-OOA and strongly oxidised, older LV-OOA) were identified, while during the colder season only strongly oxidised OOA was found.

Typical tracers for anthropogenic emissions (CO_2, NO_x, PAH, HOA, COA) were increased at the urban measurement location. However, absolute concentrations of POA were higher at the suburban location, due to a strong contribution from biomass burning OA, which here accounted for 1.28 µg m^{-3} (24 % of total OA) and for 0.82 µg m^{-3} (18 % of total OA) in Oct/Nov 2013 and May/June 2014, respectively. To a large degree this was related to agricultural waste burning in the surrounding areas and during Oct/Nov2013 potentially also to residential wood burning in the urban periphery.

Cooking- and traffic-related aerosol was observed at both locations during both seasons. The diurnal cycles of HOA (traffic-related OA) always peaked during rush hour times. A time shift in the morning rush hour peak between the suburban site and central Rome was observed, likely as a consequence of traffic progressing from the suburbs to the city centre. HOA accounted for 0.59 to 0.93 µg m^{-3} (13 to 29 % of OA) at the different locations and seasons. COA, as an indicator for cooking activities, showed maximum concentrations during lunch and dinner times at central Rome, whereas at the suburban location only during dinner times distinct peaks were observed. Average COA mass concentrations of 0.45 to 0.70 µg m^{-3} (8 to 29 % of OA) were found, with higher concentrations observed at central Rome compared to the suburban location (2013: +50 %; 2014: +23 %), as expected due to the higher density of related sources.

A type of OA related to nearby cigarette emissions (CSOA) was detected at central Rome, and found to strongly correlate with a characteristic nicotine fragment (*N*-methylpyrrolidine, $C_5H_{10}N^+$) at *m/z* 84 in the mass spectra. This ion could serve as a suitable tracer for locally emitted cigarette smoke also for other datasets. However, in order to identify CSOA based solely on this tracer ion, CSOA must account for at least 10 % of the sum of COA, HOA and BBOA, due to interferences of neighbouring ion signals from these POA types. In the absence of those, a detection limit of 80 ng m^{-3} was found for CSOA. These findings imply that the resolution of the HR-AMS is not sufficient to identify urban background contributions of cigarette emissions (~1 % of PM_1, Rogge et al., 1994) based solely on $C_5H_{10}N^+$, while fitting of this ion could be worthwhile for HR-AMS datasets which are potentially influenced by nearby cigarette emissions.

During our measurements sub-micron aerosol originating from sources in the metropolitan area of Rome and particles being advected from outside (dust periods were excluded) contributed 42-70 % and 30-58 % to total measured PM_1, respectively. Thus, during our measurements approximately half of the locally measured PM_1 was “home-made”.

While for individual aerosol types clear spatial and temporal characteristics were observed and can be understood, no general conclusion can be drawn whether total aerosol mass concentrations are generally higher at the suburb or the city centre. Instead, consistent with observations made in the area of Paris (Freutel et al., 2013), it was found that aerosol levels strongly depend on the combination of meteorological conditions (e.g. origin of air masses, dilution capacity within the boundary layer) and contributions of secondary aerosols and local emissions.

Acknowledgements

The authors thank F. Barnaba, L. Di Liberto, F. Costabile and D. Dionisi of the DIAPASON team for their support and cooperation during and after the campaigns. We gratefully thank Thomas Böttger, Antonios Dragoneas and the hospital Santo Spirito in Sassia for logistical and technical support during the field campaigns. We also thank the Arpa Lazio Environmental Agency for providing TKE data, the Barcelona Supercomputing Center for providing the BSC-DREAM8b model outputs, and NOAA Air Resources Laboratory (ARL) for the provision of the HYSPLIT transport and dispersion model. Franziska Köllner and Daniel Kunkel are gratefully acknowledged for providing the FLEXPART data. We thank anonymous reviewer #2 for helpful comments regarding *m/z* 42 as potential nicotine tracer.

References

Aiken, A. C., DeCarlo, P. F., and Jimenez, J. L.: Elemental analysis of organic species with electron ionization high-resolution mass spectrometry, Analytical Chemistry, 79, 8350-8358, 2007.

Alam, A., Shi, J. P., and Harrison, R. M.: Observations of new particle formation in urban air, J. Geophys. Res.-Atmos., 108, 2003.

Alfarra, M. R., Coe, H., Allan, J. D., Bower, K. N., Boudries, H., Canagaratna, M. R., Jimenez, J. L., Jayne, J. T., Garforth, A. A., Li, S. M., and Worsnop, D. R.: Characterization of urban and rural organic particulate in the lower Fraser valley using two aerodyne aerosol mass spectrometers, Atmos. Environ., 38, 5745-5758, 2004.

Allan, J. D., Williams, P. I., Morgan, W. T., Martin, C. L., Flynn, M. J., Lee, J., Nemitz, E., Phillips, G. J., Gallagher, M. W., and Coe, H.: Contributions from transport, solid fuel burning and cooking to primary organic aerosols in two UK cities, Atmos. Chem. Phys., 10, 647-668, 2010.

Alpert, P., Krichak, S. O., Tsidulko, M., Shafir, H., and Joseph, J. H.: A dust prediction system with TOMS initialization, Monthly Weather Review, 130, 2335-2345, 2002.

Angelini, F. and Gobbi, G. P.: Some remarks about lidar data preprocessing and different implementations of the gradient method for determining the aerosol layers, Annals of Geophysics, 57, 2014.

Barnaba, F., Bolignano, A., Di Liberto, L., Morelli, M., Lucarelli, F., Nava, S., Perrino, C., Canepari, S., Basart, S., Costabile , F., Dionisi, D., Ciampichetti, S., Sozzi, R., and Gobbi, G. P.: Desert dust contribution to PM10 levels in Italy: results from an automated method building on and upgrading the relevant European Commission Guidelines in support to the Air Quality Directive 2008/50, in preparation 2016.

Barnaba, F. and Gobbi, G. P.: Aerosol seasonal variability over the Mediterranean region and relative impact of maritime, continental and Saharan dust particles over the basin from MODIS data in the year 2001, Atmos. Chem. Phys., 4, 2367–2391, 2004.

Basart, S., Perez, C., Nickovic, S., Cuevas, E., and Maria Baldasano, J.: Development and evaluation of the BSC-DREAM8b dust regional model over Northern Africa, the Mediterranean and the Middle East, Tellus Ser. B-Chem. Phys. Meteorol., 64, 2012.

Boucher, O., Randall, D., Artaxo, P., Bretherton, C., Feingold, G., Forster, P., Kerminen, V.-M., Kondo, Y., Liao, H., Lohmann, U., Rasch, P., Satheesh, S. K., Sherwood, S., Stevens, B., and Zhang, X. Y.: 2013: Clouds and Aerosols. In: Climate Change 2013: The Physical Science Basis. Contribution of Working Group I to the Fifth Assessment Report of the Intergovernmental Panel on Climate Change, Cambridge, United Kingdom and New York, NY, USA, 2013.

Bougiatioti, A., Stavroulas, I., Kostenidou, E., Zarmpas, P., Theodosi, C., Kouvarakis, G., Canonaco, F., Prévôt, A. S. H., Nenes, A., Pandis, S. N., and Mihalopoulos, N.: Processing of biomass-burning aerosol in the eastern Mediterranean during summertime, Atmos. Chem. Phys., 14, 4793-4807, 2014.

Brines, M., Dall'Osto, M., Beddows, D. C. S., Harrison, R. M., Gomez-Moreno, F., Nunez, L., Artinano, B., Costabile, F., Gobbi, G. P., Salimi, F., Morawska, L., Sioutas, C., and Querol, X.: Traffic and nucleation events as main sources of ultrafine particles in high-insolation developed world cities, Atmos. Chem. Phys., 15, 5929-5945, 2015.

Canagaratna, M. R., Jayne, J. T., Jimenez, J. L., Allan, J. D., Alfarra, M. R., Zhang, Q., Onasch, T. B., Drewnick, F., Coe, H., Middlebrook, A., Delia, A., Williams, L. R., Trimborn,

A. M., Northway, M. J., DeCarlo, P. F., Kolb, C. E., Davidovits, P., and Worsnop, D. R.: Chemical and microphysical characterization of ambient aerosols with the aerodyne aerosol mass spectrometer, Mass Spectrometry Reviews, 26, 185-222, 2007.

Canagaratna, M. R., Jimenez, J. L., Kroll, J. H., Chen, Q., Kessler, S. H., Massoli, P., Ruiz, L. H., Fortner, E., Williams, L. R., Wilson, K. R., Surratt, J. D., Donahue, N. M., Jayne, J. T., and Worsnop, D. R.: Elemental ratio measurements of organic compounds using aerosol mass spectrometry: characterization, improved calibration, and implications, Atmos. Chem. Phys., 15, 253-272, 2015.

Carslaw, D. C., Beevers, S. D., Ropkins, K., and Bell, M. C.: Detecting and quantifying aircraft and other on-airport contributions to ambient nitrogen oxides in the vicinity of a large international airport, Atmos. Environ., 40, 5424-5434, 2006.

Costabile, F., Amoroso, A., and Wang, F.: Sub-µm particle size distributions in a suburban Mediterranean area. Aerosol populations and their possible relationship with HONO mixing ratios, Atmos. Environ., 44, 5258-5268, 2010.

Crippa, M., DeCarlo, P. F., Slowik, J. G., Mohr, C., Heringa, M. F., Chirico, R., Poulain, L., Freutel, F., Sciare, J., Cozic, J., Di Marco, C. F., Elsasser, M., Nicolas, J. B., Marchand, N., Abidi, E., Wiedensohler, A., Drewnick, F., Schneider, J., Borrmann, S., Nemitz, E., Zimmermann, R., Jaffrezo, J. L., Prevot, A. S. H., and Baltensperger, U.: Wintertime aerosol chemical composition and source apportionment of the organic fraction in the metropolitan area of Paris, Atmos. Chem. Phys., 13, 961-981, 2013a.

Crippa, M., El Haddad, I., Slowik, J. G., DeCarlo, P. F., Mohr, C., Heringa, M. F., Chirico, R., Marchand, N., Sciare, J., Baltensperger, U., and Prevot, A. S. H.: Identification of marine and continental aerosol sources in Paris using high resolution aerosol mass spectrometry, J. Geophys. Res.-Atmos., 118, 1950-1963, 2013b.

DeCarlo, P. F., Kimmel, J. R., Trimborn, A., Northway, M. J., Jayne, J. T., Aiken, A. C., Gonin, M., Fuhrer, K., Horvath, T., Docherty, K. S., Worsnop, D. R., and Jimenez, J. L.: Field-Deployable, High-Resolution, Time-of-Flight Aerosol Mass Spectrometer, Analytical Chemistry, 78, 8281-8289, 2006.

DeCarlo, P. F., Ulbrich, I. M., Crounse, J., de Foy, B., Dunlea, E. J., Aiken, A. C., Knapp, D., Weinheimer, A. J., Campos, T., Wennberg, P. O., and Jimenez, J. L.: Investigation of the sources and processing of organic aerosol over the Central Mexican Plateau from aircraft measurements during MILAGRO, Atmos. Chem. Phys., 10, 5257-5280, 2010.

DIAPASON: available at: http://www.diapason-life.eu/index.php?option=com_content&view=article&id=171&Itemid=466&lang=en, last access: 11.11.2016.

Drewnick, F., Boettger, T., von der Weiden-Reinmueller, S. L., Zorn, S. R., Klimach, T., Schneider, J., and Borrmann, S.: Design of a mobile aerosol research laboratory and data processing tools for effective stationary and mobile field measurements, Atmospheric Measurement Techniques, 5, 1443-1457, 2012.

Faber, P., Drewnick, F., Veres, P. R., Williams, J., and Borrmann, S.: Anthropogenic sources of aerosol particles in a football stadium: Real-time characterization of emissions from cigarette smoking, cooking, hand flares, and color smoke bombs by high-resolution aerosol mass spectrometry, Atmos. Environ., 77, 1043-1051, 2013.

Freutel, F., Schneider, J., Drewnick, F., von der Weiden-Reinmuller, S. L., Crippa, M., Prevot, A. S. H., Baltensperger, U., Poulain, L., Wiedensohler, A., Sciare, J., Sarda-Esteve, R., Burkhart, J. F., Eckhardt, S., Stohl, A., Gros, V., Colomb, A., Michoud, V., Doussin, J. F., Borbon, A., Haeffelin, M., Morille, Y., Beekmann, M., and Borrmann, S.: Aerosol particle measurements at three stationary sites in the megacity of Paris during summer 2009: meteorology and air mass origin dominate aerosol particle composition and size distribution, Atmos. Chem. Phys., 13, 933-959, 2013.

Fröhlich, R., Cubison, M. J., Slowik, J. G., Bukowiecki, N., Canonaco, F., Croteau, P. L., Gysel, M., Henne, S., Herrmann, E., Jayne, J. T., Steinbacher, M., Worsnop, D. R., Baltensperger, U., and Prévôt, A. S. H.: Fourteen months of on-line measurements of the non-refractory submicron aerosol at the Jungfraujoch (3580 m a.s.l.) – chemical composition, origins and organic aerosol sources, Atmos. Chem. Phys., 15, 11373-11398, 2015.

Fuller, G. W., Sciare, J., Lutz, M., Moukhtar, S., and Wagener, S.: New Directions: Time to tackle urban wood burning?, Atmos. Environ., 68, 295-296, 2013.

Fuzzi, S., Baltensperger, U., Carslaw, K., Decesari, S., van der Gon, H. D., Facchini, M. C., Fowler, D., Koren, I., Langford, B., Lohmann, U., Nemitz, E., Pandis, S., Riipinen, I., Rudich, Y., Schaap, M., Slowik, J. G., Spracklen, D. V., Vignati, E., Wild, M., Williams, M., and

Gilardoni, S.: Particulate matter, air quality and climate: lessons learned and future needs, Atmos. Chem. Phys., 15, 8217-8299, 2015.

Gariazzo, C., Argentini, S., Balducci, C., Bogliolo, M. P., Cecinato, A., Cesaroni, G., Cristofari, A., D'Allura, A., Finardi, S., Forastiere, F., Gatto, M. P., Gherardi, M., Gordiani, A., Hänninen, O., Lamberti, M., Pelliccioni, A., Perilli, M., Perrino, C., Porta, D., Radice, P., Romagnoli, P., Sacco, F., Silibello, C., Stafoggia, M., and Tofful, L.: Biomass burning contribution to PAHs concentration in the urban area of Rome. Main findings from the LIFE+ EXPAH project and further observations., 10th International Conference on Air Quality - Science and Application, Milan, Italy, 2016.

Gobbi, G. P., Angelini, F., Barnaba, F., Costabile, F., Baldasano, J. M., Basart, S., Sozzi, R., and Bolignano, A.: Changes in particulate matter physical properties during Saharan advections over Rome (Italy): a four-year study, 2001-2004, Atmos. Chem. Phys., 13, 7395-7404, 2013.

Gobbi, G. P., Barnaba, F., and Ammannato, L.: The vertical distribution of aerosols, Saharan dust and cirrus clouds in Rome (Italy) in the year 2001, Atmos. Chem. Phys., 4, 351–359, 2004.

Harrison, R. M., Grenfell, J. L., Savage, N., Allen, A., Clemitshaw, K. C., Penkett, S., Hewitt, C. N., and Davison, B.: Observations of new particle production in the atmosphere of a moderately polluted site in eastern England, J. Geophys. Res.-Atmos., 105, 17819-17832, 2000.

Heal, M. R., Kumar, P., and Harrison, R. M.: Particles, air quality, policy and health, Chemical Society Reviews, 41, 6606-6630, 2012.

Hildemann, L. M., Markowski, G. R., and Cass, G. R.: Chemical composition of emissions from urban sources of fine organic aerosol, Environ. Sci. Technol., 25, 744-759, 1991.

Jacob III, P. and Byrd, G. D.: Chapter 6 - Use of gas chromatographic and mass spectrometric techniques for the determination of nicotine and its metabolites. In: Analytical Determination of Nicotine and Related Compounds and their Metabolites, Elsevier Science, Amsterdam, 1999.

Jayne, J. T., Leard, D. C., Zhang, X., Davidovits, P., Smith, K. A., Kolb, C. E., and D.R.Worsnop: Development of an Aerosol Mass Spectrometer for Size and Composition Analysis of Submicron Particles, Aerosol Science and Technology, 33, 49-70, 2000.

Jimenez, J. L., Canagaratna, M. R., Donahue, N. M., Prevot, A. S. H., Zhang, Q., Kroll, J. H., DeCarlo, P. F., Allan, J. D., Coe, H., Ng, N. L., Aiken, A. C., Docherty, K. S., Ulbrich, I. M., Grieshop, A. P., Robinson, A. L., Duplissy, J., Smith, J. D., Wilson, K. R., Lanz, V. A., Hueglin, C., Sun, Y. L., Tian, J., Laaksonen, A., Raatikainen, T., Rautiainen, J., Vaattovaara, P., Ehn, M., Kulmala, M., Tomlinson, J. M., Collins, D. R., Cubison, M. J., Dunlea, E. J., Huffman, J. A., Onasch, T. B., Alfarra, M. R., Williams, P. I., Bower, K., Kondo, Y., Schneider, J., Drewnick, F., Borrmann, S., Weimer, S., Demerjian, K., Salcedo, D., Cottrell, L., Griffin, R., Takami, A., Miyoshi, T., Hatakeyama, S., Shimono, A., Sun, J. Y., Zhang, Y. M., Dzepina, K., Kimmel, J. R., Sueper, D., Jayne, J. T., Herndon, S. C., Trimborn, A. M., Williams, L. R., Wood, E. C., Middlebrook, A. M., Kolb, C. E., Baltensperger, U., and Worsnop, D. R.: Evolution of Organic Aerosols in the Atmosphere, Science, 326, 1525-1529, 2009.

Kallos, G., Nickovic, S., Papadopoulos, A., Jovic, D., Kakaliagou, O., Misirlis, N., Boukas, L., Mimikou, N., Sakellaridis, G., Papageorgiou, J., Anadranistakis, E., and Manousakis, M.: The regional weather forecasting system SKIRON: An overview, paper presented at the International Symposium on Regional Weather Prediction on Parallel Computer Environments, University of Athens, Athens, Greece, 15-17 Oct. 1997.

Kulmala, M. and Kerminen, V.-M.: On the formation and growth of atmospheric nanoparticles, Atmospheric Research, 90, 132-150, 2008.

Lanz, V. A., Alfarra, M. R., Baltensperger, U., Buchmann, B., Hueglin, C., and Prevot, A. S. H.: Source apportionment of submicron organic aerosols at an urban site by factor analytical modelling of aerosol mass spectra, Atmos. Chem. Phys., 7, 1503-1522, 2007.

Lanz, V. A., Prevot, A. S. H., Alfarra, M. R., Weimer, S., Mohr, C., DeCarlo, P. F., Gianini, M. F. D., Hueglin, C., Schneider, J., Favez, O., D'Anna, B., George, C., and Baltensperger, U.: Characterization of aerosol chemical composition with aerosol mass spectrometry in Central Europe: an overview, Atmos. Chem. Phys., 10, 10453-10471, 2010.

Lucarelli, F., Calzolai, G., Chiari, M., Giannoni, M., Mochi, D., Nava, S., and Carraresi, L.: The upgraded external-beam PIXE/PIGE set-up at LABEC for very fast measurements on aerosol samples, Nuclear Instruments & Methods in Physics Research Section B-Beam Interactions with Materials and Atoms, 318, 55-59, 2014.

Minguillon, M. C., Brines, M., Perez, N., Reche, C., Pandolfi, M., Fonseca, A. S., Amato, F., Alastuey, A., Lyasota, A., Codina, B., Lee, H. K., Eun, H. R., Ahn, K. H., and Querol, X.: New particle formation at ground level and in the vertical column over the Barcelona area, Atmospheric Research, 164, 118-130, 2015.

Mohr, C., DeCarlo, P. F., Heringa, M. F., Chirico, R., Slowik, J. G., Richter, R., Reche, C., Alastuey, A., Querol, X., Seco, R., Penuelas, J., Jimenez, J. L., Crippa, M., Zimmermann, R., Baltensperger, U., and Prevot, A. S. H.: Identification and quantification of organic aerosol from cooking and other sources in Barcelona using aerosol mass spectrometer data, Atmos. Chem. Phys., 12, 1649-1665, 2012.

Mohr, C., Huffman, J. A., Cubison, M. J., Aiken, A. C., Docherty, K. S., Kimmel, J. R., Ulbrich, I. M., Hannigan, M., and Jimenez, J. L.: Characterization of Primary Organic Aerosol Emissions from Meat Cooking, Trash Burning, and Motor Vehicles with High-Resolution Aerosol Mass Spectrometry and Comparison with Ambient and Chamber Observations, Environ. Sci. Technol., 43, 2443-2449, 2009.

Nava, S., Becagli, S., Calzolai, G., Chiari, M., Lucarelli, F., Prati, P., Traversi, R., Udisti, R., Valli, G., and Vecchi, R.: Saharan dust impact in central Italy: An overview on three years elemental data records, Atmos. Environ., 60, 444-452, 2012.

Ng, N. L., Canagaratna, M. R., Zhang, Q., Jimenez, J. L., Tian, J., Ulbrich, I. M., Kroll, J. H., Docherty, K. S., Chhabra, P. S., Bahreini, R., Murphy, S. M., Seinfeld, J. H., Hildebrandt, L., Donahue, N. M., DeCarlo, P. F., Lanz, V. A., Prevot, A. S. H., Dinar, E., Rudich, Y., and Worsnop, D. R.: Organic aerosol components observed in Northern Hemispheric datasets from Aerosol Mass Spectrometry, Atmos. Chem. Phys., 10, 4625-4641, 2010.

Paatero, P. and Tapper, U.: Positive matrix factorization: A non-negative factor model with optimal utilization of error estimates of data values, Environmetrics, 5, 111-126, 1994.

Perez, C., Nickovic, S., Baldasano, J. M., Sicard, M., Rocadenbosch, F., and Cachorro, V. E.: A long Saharan dust event over the western Mediterranean: Lidar, Sun photometer observations, and regional dust modeling, J. Geophys. Res.-Atmos., 111, 2006a.

Perez, C., Nickovic, S., Pejanovic, G., Baldasano, J. M., and Oezsoy, E.: Interactive dust-radiation modeling: A step to improve weather forecasts, J. Geophys. Res.-Atmos., 111, 2006b.

Pikridas, M., Sciare, J., Freutel, F., Crumeyrolle, S., von der Weiden-Reinmüller, S. L., Borbon, A., Schwarzenboeck, A., Merkel, M., Crippa, M., Kostenidou, E., Psichoudaki, M., Hildebrandt, L., Engelhart, G. J., Petäjä, T., Prévôt, A. S. H., Drewnick, F., Baltensperger, U., Wiedensohler, A., Kulmala, M., Beekmann, M., and Pandis, S. N.: In situ formation and spatial variability of particle number concentration in a European megacity, Atmos. Chem. Phys., 15, 10219-10237, 2015.

Reche, C., Querol, X., Alastuey, A., Viana, M., Pey, J., Moreno, T., Rodriguez, S., Gonzalez, Y., Fernandez-Camacho, R., Sanchez de la Campa, A. M., de la Rosa, J., Dall'Osto, M., Prevot, A. S. H., Hueglin, C., Harrison, R. M., and Quincey, P.: New considerations for PM, Black Carbon and particle number concentration for air quality monitoring across different European cities, Atmos. Chem. Phys., 11, 6207-6227, 2011.

Reche, C., Viana, M., Amato, F., Alastuey, A., Moreno, T., Hillamo, R., Teinila, K., Saarnio, K., Seco, R., Penuelas, J., Mohr, C., Prevot, A. S. H., and Querol, X.: Biomass burning contributions to urban aerosols in a coastal Mediterranean City, Sci. Total Environ., 427, 175-190, 2012.

Rizza, U., Barnaba, F., Miglietta, M. M., Gobbi, G. P., Mangia, C., Di Liberto, L., Dionisi, D., Costabile, F., and Grasso, F.: WRF-Chem model simulations of a dust outbreak over the Central Mediterranean and comparison with multi-sensor desert dust observations, Atmos. Chem. Phys. Discuss., 2016, 1-37, 2016.

Rogge, W. F., Hildemann, L. M., Mazurek, M. A., and Cass, G. R.: Sources of Fine Organic Aerosol. 6. Cigarette Smoke in the Urban Atmosphere, Environ. Sci. Technol., 28, 1375-1388, 1994.

Schneider, J., Weimer, S., Drewnick, F., Borrmann, S., Helas, G., Gwaze, P., Schmid, O., Andreae, M. O., and Kirchner, U.: Mass spectrometric analysis and aerodynamic properties of various types of combustion-related aerosol particles, International Journal of Mass Spectrometry, 258, 37-49, 2006.

Shi, J. P., Evans, D. E., Khan, A. A., and Harrison, R. M.: Sources and concentration of nanoparticles (< 10 nm diameter) in the urban atmosphere, Atmos. Environ., 35, 1193-1202, 2001.

Sibson, R.: A brief description of natural neighbour interpolation. In: Interpreting Multivariate Data, Barnett, I. V. (Ed.), Wiley, New York, USA, 1981.

Srivastava, M. K. and Sarthi, P. P.: Turbulent kinetic energy in the atmospheric surface layer during the summer monsoon, Meteorological Applications, 9, 239-246, 2002.

Stafoggia, M., Zauli-Sajani, S., Pey, J., Samoli, E., Alessandrini, E., Basagana, X., Cernigliaro, A., Chiusolo, M., Demaria, M., Diaz, J., Faustini, A., Katsouyanni, K., Kelessis, A. G., Linares, C., Marchesi, S., Medina, S., Pandolfi, P., Perez, N., Querol, X., Randi, G., Ranzi, A., Tobias, A., Forastiere, F., and Grp, M.-P. S.: Desert Dust Outbreaks in Southern Europe: Contribution to Daily PM10 Concentrations and Short-Term Associations with Mortality and Hospital Admissions, Environmental Health Perspectives, 124, 413-419, 2016.

Stein, A. F., Draxler, R. R., Rolph, G. D., Stunder, B. J. B., Cohen, M. D., and Ngan, F.: NOAA's HYSPLIT Atmospheric Transport and Dispersion Modeling System, Bulletin of the American Meteorological Society, 96, 2059-2077, 2015.

Stohl, A., Forster, C., Frank, A., Seibert, P., and Wotawa, G.: Technical note: The Lagrangian particle dispersion model FLEXPART version 6.2, Atmos. Chem. Phys., 5, 2461-2474, 2005.

Ulbrich, I. M., Canagaratna, M. R., Zhang, Q., Worsnop, D. R., and Jimenez, J. L.: Interpretation of organic components from Positive Matrix Factorization of aerosol mass spectrometric data, Atmos. Chem. Phys., 9, 2891-2918, 2009.

Weimer, S., Alfarra, M. R., Schreiber, D., Mohr, M., Prevot, A. S. H., and Baltensperger, U.: Organic aerosol mass spectral signatures from wood-burning emissions: Influence of burning conditions and wood type, J. Geophys. Res.-Atmos., 113, 2008.

Yu, K. N., Cheung, Y. P., Cheung, T., and Henry, R. C.: Identifying the impact of large urban airports on local air quality by nonparametric regression, Atmos. Environ., 38, 4501-4507, 2004.

Zhang, Q., Jimenez, J. L., Canagaratna, M. R., Ulbrich, I. M., Ng, N. L., Worsnop, D. R., and Sun, Y.: Understanding atmospheric organic aerosols via factor analysis of aerosol mass spectrometry: a review, Anal. Bioanal. Chem., 401, 3045-3067, 2011.

Zhang, Q., Stanier, C. O., Canagaratna, M. R., Jayne, J. T., Worsnop, D. R., Pandis, S. N., and Jimenez, J. L.: Insights into the chemistry of new particle formation and growth events in Pittsburgh based on aerosol mass spectrometry, Environ. Sci. Technol., 38, 4797-4809, 2004.

Zheng, M., Salmon, L. G., Schauer, J. J., Zeng, L. M., Kiang, C. S., Zhang, Y. H., and Cass, G. R.: Seasonal trends in PM2.5 source contributions in Beijing, China, Atmos. Environ., 39, 3967-3976, 2005.

Table 1. Summary of measurement campaigns and measurement periods.

Campaign name	Measurement location	Classification	Measurement period
DIAPASON2013	Tor Vergata	Urban background	23.10. – 07.11.2013
POPE2013	Central Rome	Urban	07.11. – 14.11.2013
DIAPASON2014	Tor Vergata	Urban background	20.05. – 04.06.2014
POPE2014	Central Rome	Urban	04.06. – 17.06.2014

Table 2. Summary of the instruments deployed in MoLa during all measurement periods, together with measured variables. D_p: particle diameter (defined according to individual instrumental measurement method: optical, aerodynamic, or mobility diameter).

Instrument	Measured variable
Chemical composition of PM_1	
Aerosol mass spectrometer (HR-ToF-AMS)	Organics, sulphate, nitrate, ammonium, chloride (non-refractory) mass concentrations (D_p = ~ 70 – 800 nm)
Multi Angle Absorption Photometer (MAAP)	Black carbon (BC) mass concentration
PAS2000	Particulate PAH[a] mass concentration
Physical aerosol properties	
Condensation particle counter (CPC)	Total number concentration (D_p > 2.5 nm)
Fast mobility particle sizer (FMPS)	Size distribution (D_p = 5.6 – 560 nm)
Optical particle counter (OPC)[b]	Size distribution (D_p = 0.25 – 32 µm)
Aerodynamic particle sizer (APS)	Size distribution (D_p = 0.5 – 20 µm)
Environmental Dust Monitor (EDM)	Mass concentration of PM_1, $PM_{2.5}$, PM_{10}
Trace gas mixing ratios	
Airpointer	NO_2, NO_x, NO, SO_2, CO, O_3
LI-840	H_2O, CO_2
Meteorology	
Meteorological station[c]	Wind direction, wind speed, temperature, pressure, solar radiation, precipitation, relative humidity

[a] Polycyclic Aromatic Hydrocarbons

[b] No data collected during DIAPASON2014.

[c] Wind direction, wind speed and solar radiation data not useable during POPE measurements.

Table 3. Summary of selected variables measured during DIAPASON (Tor Vergata) and POPE (central Rome) in 2013 and 2014. Values represent total campaign averages, calculated from 5 min averages, and their standard deviations. N/A: not available.

	DIAPASON2013 (Oct/Nov 2013)	POPE2013 (Nov 2013)	DIAPASON2014 (May/June 2014)	POPE2014 (June 2014)
Temperature / °C	17.6 ± 2.9	16.1 ± 2.8	19.0 ± 3.5	24.9 ± 4.5
Rain [a] / mm	46.3 (5)	25.9 (6)	6.3 (5)	69.9 (4)
Pressure / hPa	1004 ± 7	1009 ± 6	1002 ± 2	1012 ± 4
Solar radiation [b] / W m^{-2}	103 ± 26	N/A	282 ± 55	N/A
Rel. humidity / %	78 ± 11	73 ± 6	61 ± 15	52 ± 16
Wind speed / m s^{-1}	1.9 ± 1.3	N/A	2.5 ± 1.6	N/A
Daily BLH [c] max. / m	850 ± 220	900 ± 150	1500 ± 450	1560 ± 250
TKE [d] / J kg^{-1}	0.48 ± 0.45	1.8 ± 2.3	0.84 ± 0.79	0.68 ± 0.52
PM_{10} [e] / µg m^{-3}	22 ± 12	13 ± 7	15 ± 8	17 ± 8
$PM_{10-2.5}$ [e,f] / µg m^{-3}	4.5 ± 3.1	4.7 ± 3.2	9.3 ± 6.5	7.1 ± 5.7
PM_1 [e] / µg m^{-3}	15 ± 10	6.0 ± 3.6	5.8 ± 3.5	7.5 ± 3.8
PM_1 (AMS+BC) [g,i] / µg m^{-3}	12 ± 8	5.6 ± 4	8.7 ± 5	12.5 ± 6
PNC [h] / 10^3 cm^{-3}	23 ± 15	27 ± 11	18 ± 10	13 ± 5
NO_x / ppb	29 ± 27	36 ± 27	9 ± 9	13 ± 8
CO_2 / ppm	410 ± 20	420 ± 20	410 ± 20	420 ± 20
O_3 / ppb	14 ± 14	8.9 ± 10	34 ± 19	35 ± 22
PAH / ng m^{-3}	45 ± 54	45 ± 39	10 ± 14	12 ± 11
Org [~~f~~i] / µg m^{-3}	5.3 ± 4.5	2.5 ± 1.8	4.5 ± 3.2	6.6 ± 3.3

SO_4 / µg m^{-3}	2.0 ± 1.1	0.48 ± 0.44	1.6 ± 0.44	2.6 ± 1.3
NO_3 / µg m^{-3}	0.86 ± 0.80	0.23 ± 0.17	0.61 ± 0.72	0.49 ± 0.40
NH_4 / µg m^{-3}	0.88 ± 0.48	0.20 ± 0.18	0.66 ± 0.27	0.97 ± 0.46
Chl / µg m^{-3}	0.09 ± 0.16	0.04 ± 0.06	0.06 ± 0.13	0.03 ± 0.08
BC / µg m^{-3}	2.9 ± 2.5	2.2 ± 1.7	1.3 ± 1.0	1.8 ± 1.0

[a] Total accumulated amount of rain during measurements. Numbers of days with rain are given in parentheses.

[b] Average and standard deviation of daily means. Only days with 24 h measurements were used (includes 85 % of data).

[c] Average and standard deviation of daily boundary layer height (BLH) maxima from polarization LIDAR-ceilometer. measurements at the Tor Vergata site provided by the DIAPASON project (DIAPASON, 2016).

[d] Turbulent kinetic energy (TKE) calculated from 2-hour averages provided by Arpa Lazio Environmental Agency from measurements at 3 sites around Rome (Tor Vergata, Castel di Guido, Boncompagni).

[e] PM concentrations from EDM measurements.

[f] Difference between PM_{10} and $PM_{2.5}$ (coarse particles).

[g] PM_1 concentration based on the sum of AMS species and BC.

[h] PNC from CPC measurements.

[i] For POPE2013 and POPE2014 corrected for contribution from local cigarette smoke emissions, compare Sect. 4.2.5.

Table 4: Estimated contribution of "home-made" and “advected” species to total PM_1 for all measurement periods. Dust advection periods and emissions from cigarettes are excluded.

	Home-made PM_1 / µg m^{-3} (contribution to PM_1 / %)	Advected PM_1 / µg m^{-3} (contribution to PM_1 / %)
DIAPASON2013	6.5 (47)	7.3 (53)
POPE2013	3.9 (70)	1.7 (30)
DIAPASON2014	4.7 (59)	3.3 (41)
POPE2014	5.2 (42)	7.3 (58)

Table 5. Summary of “dust” and “no dust” periods identified during DIAPASON2013 and DIAPASON2014, including mean values and standard deviation of $PM_{10-2.5}$ ~~and PM_{10}.~~, PM_{10} and PM_1 (all from EDM measurements).

	DIAPASON2013		**DIAPASON2014**	
	Dust	No dust	Dust	No dust
Period	~~29~~23.10. - 01.11.13	~~23.10.-28.10.13;~~ 02.11. - 07.11.13	20.05. - 26.05.14	27.05. - 04.06.14
Mean $PM_{10-2.5}$ / µg m^{-3}	~~7.1~~5.4 ± 3.~~5~~1	~~4~~3.0 ± 2.~~7~~5	15.4 ± 5.9	5.5 ± 2.8
Mean PM_{10} / µg m^{-3}	~~32 ± 7~~28 ± 10	~~19 ± 12~~11 ± 6	22 ± 7	11 ± 5
~~Fraction of PM_{10} in~~Mean PM_1 / µg m^{-3}	~~70 %~~20 ± 9 (71% of PM_{10})	~~68 %~~6.3 ± 4.1 (57% of PM_{10})	~~31 %~~7.0 ± 3.3 (32% of PM_{10})	~~48 %~~5.0 ± 3.5 (45% of PM_{10})

Table 6. Variables measured during DIAPASON2014 indicating different ambient conditions on days classified as "nucleation", "non-defined" and "non-nucleation" days. Total particle number concentrations (PNC) and the classification criteria and number of respectively classified days are also listed. For each measurement day and presented variable daily averages for the period 10 am – 4 pm were calculated. Here, mean and standard deviation of these averages are shown with maximum values coloured in red, minimum values coloured in green.

	Nucleation days	Non-defined days	Non-nucleation days
Classification	$PNC_{nuc}/PNC_{bg} \geq 1.5$	$1 < PNC_{nuc}/PNC_{bg} < 1.5$	$PNC_{nuc}/PNC_{bg} \leq 1$
Number of days	6	6	2
Rain [a] / mm	0 (0)	0.7 (1)	2.3 (1)
Total PNC / 10^3 cm^{-3}	25 ± 9	13 ± 3	12 ± 1
Temperature / ° C	23 ± 2	22 ± 2	20 ± 0
Rel. humidity / %	43 ± 6	46 ± 9	56 ± 4
Solar radiation / W m^{-2}	780 ± 80	700 ± 190	670 ± 200
O_3 / ppb	54 ± 4	47 ± 6	48 ± 1
Total PM_1 organics / µg m^{-3}	3.9 ± 2.4	3.6 ± 1.0	2.9 ± 2.3

[a] Total accumulated amount of rain (10 am – 4 pm). Numbers of days with rain are given in parentheses.

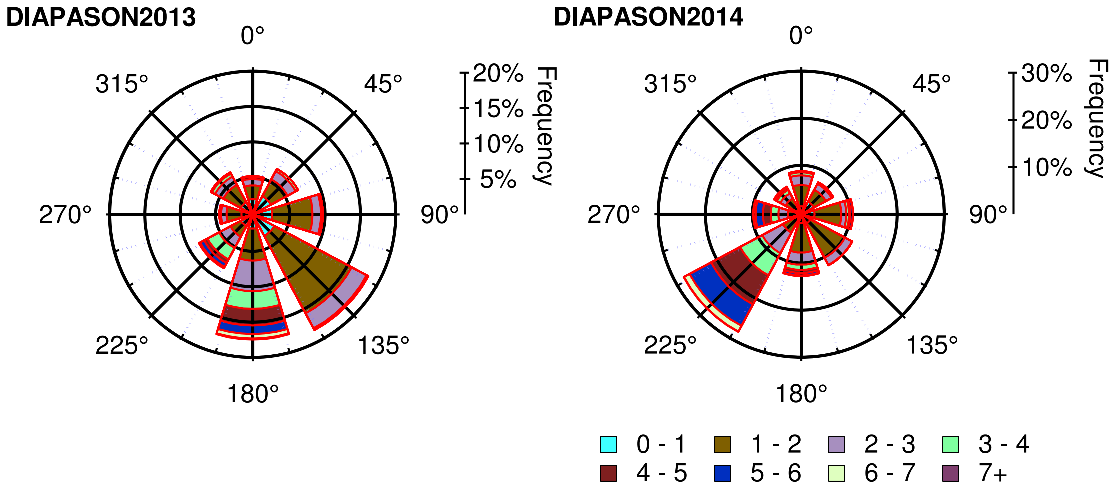

Figure 1. Relative frequency of local wind directions (in °) colour coded with wind speed measured during DIAPASON2013 (left) and DIAPASON2014 (right).

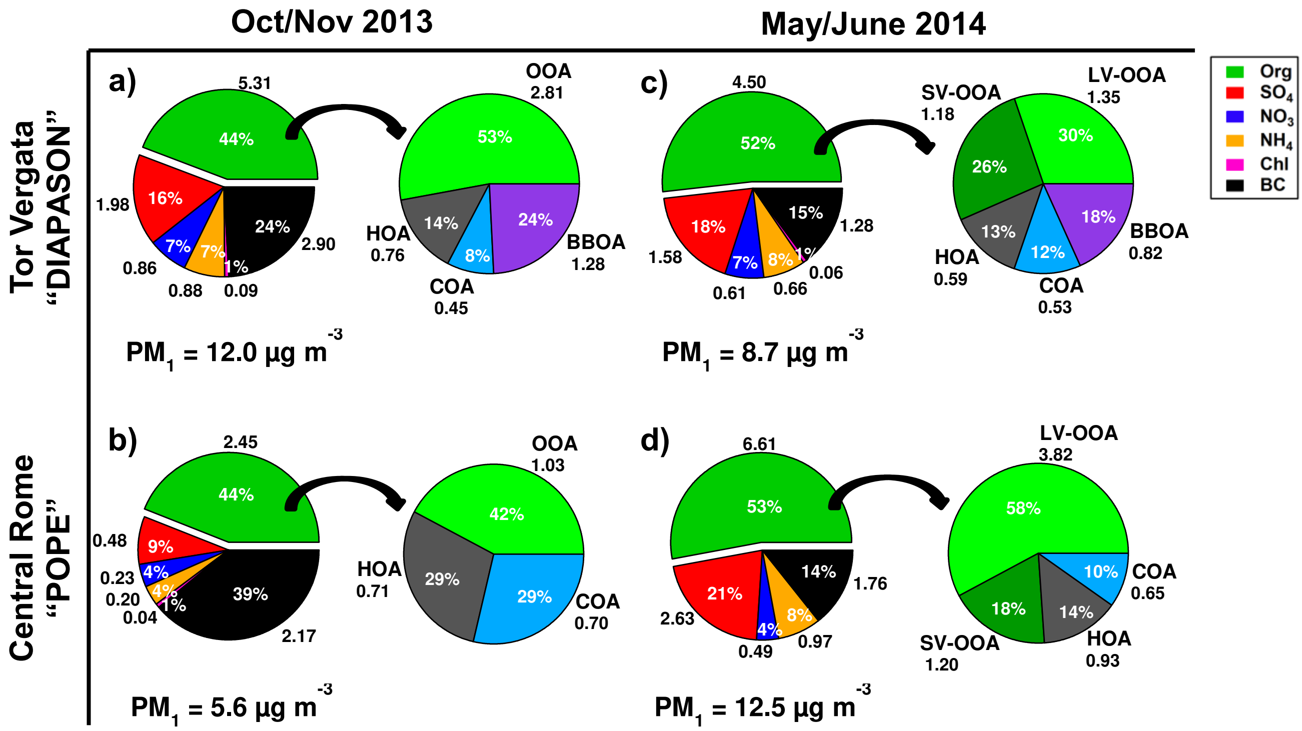

Figure 2. Mean chemical composition (µg m^{-3}) of non-refractory PM$_1$ together with BC (left chart in panels a-d) and PMF-separated organic fraction (right chart in panels a-d) for each measurement period. PM$_1$ values below the pie charts represent total mass concentration of AMS-measured species plus BC. The organic fraction measured at central Rome was corrected for contributions from cigarette smoke in the local environment (Sect. 4.2.5, also omitted from the pie charts depicting the PMF-separated organic fraction).

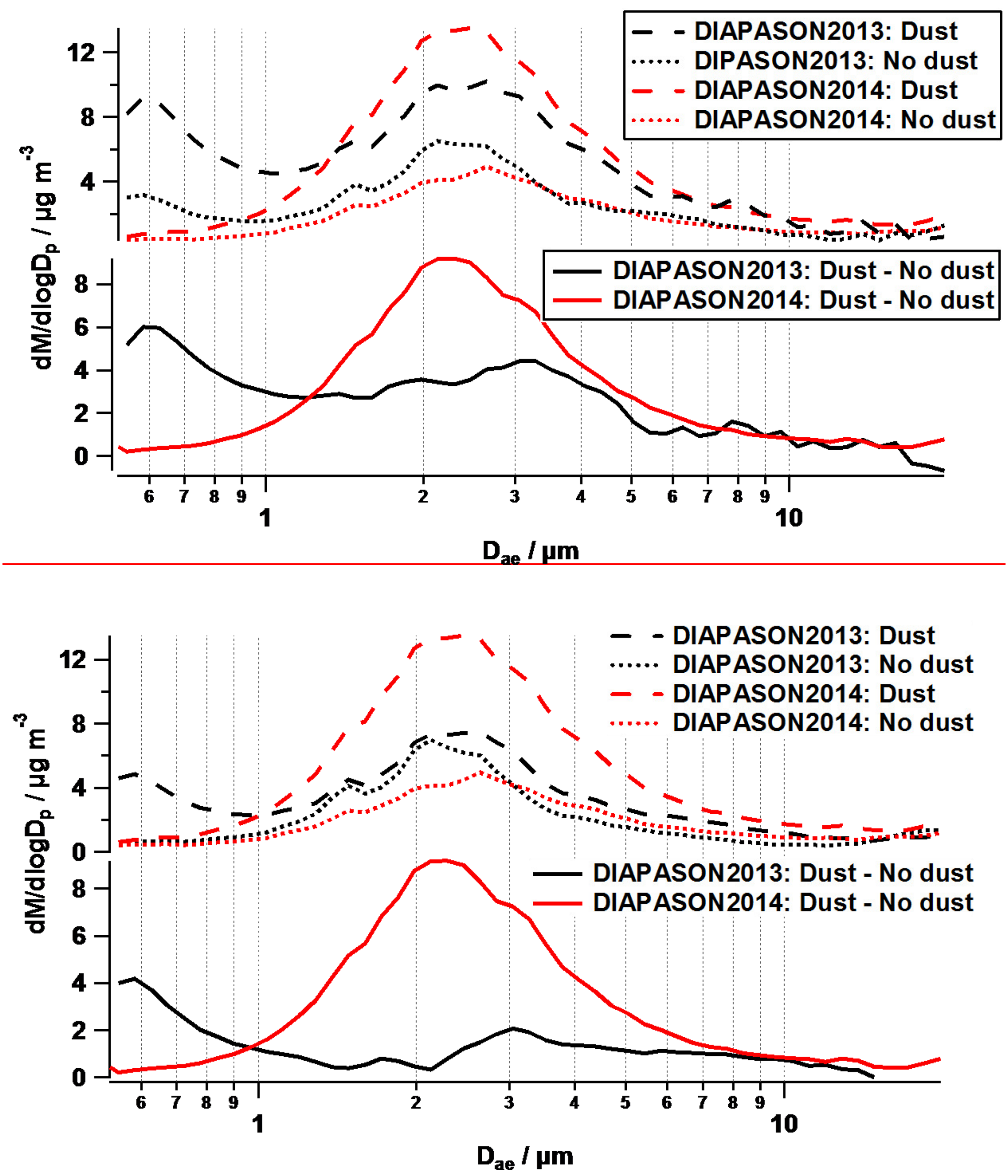

Figure 3. Size-resolved mass distribution (dM/dlogD$_p$) during "dust" (dashed traces) and "no dust" (dotted traces) periods (top panel) measured with the APS during DIAPASON2013 (black traces) and DIAPASON2014 (red traces). The difference of the size-resolved mass distributions measured during "dust" and "no dust" periods indicate the size distributions of the dust particles measured during both years (bottom panel). D$_{ae}$ is the aerodynamic particle diameter.

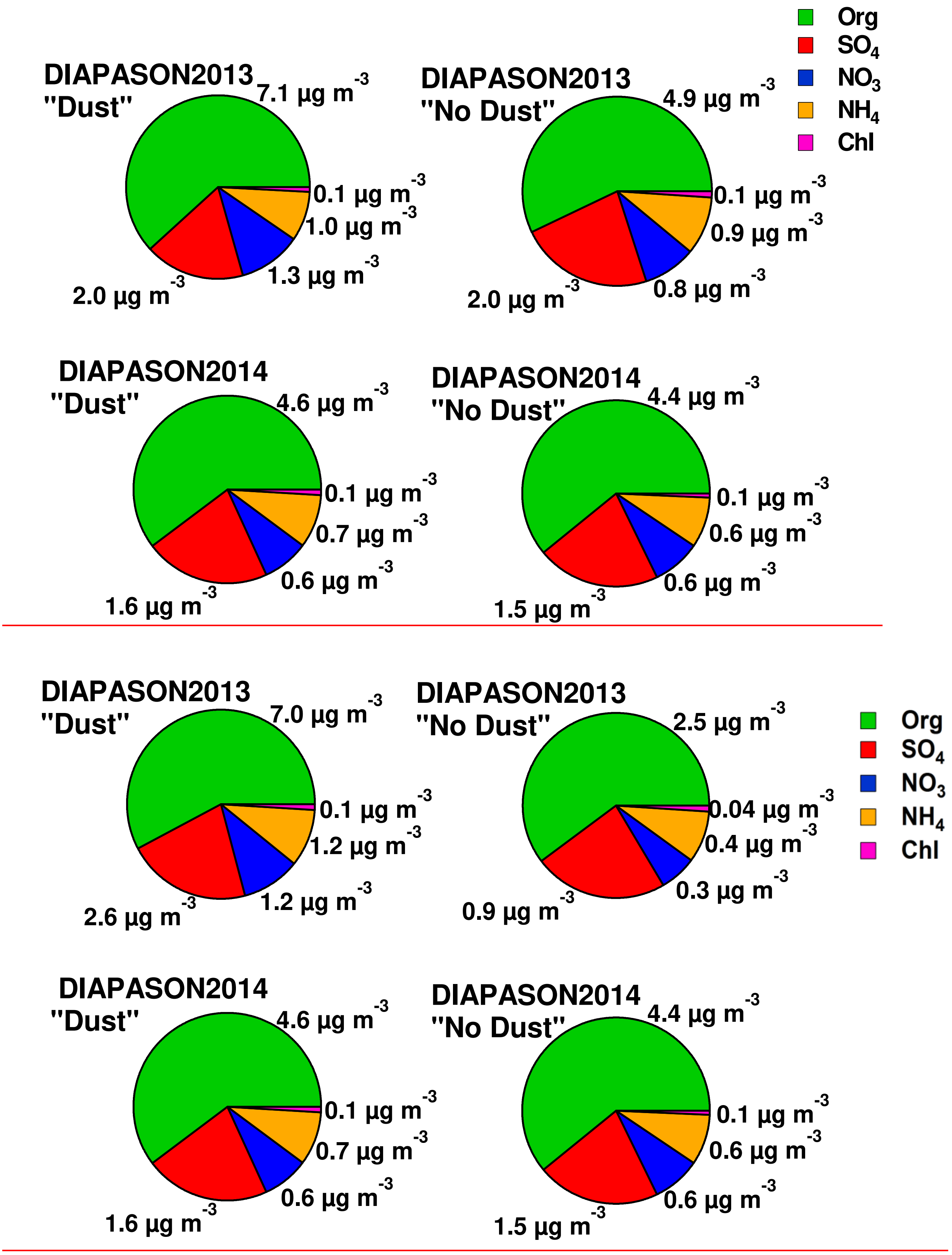

Figure 4. Comparison of mean chemical composition of non-refractory PM_1 obtained from AMS measurements during “dust” (left) and “no dust” (right) periods during DIAPASON2013 (top) and DIAPASON2014 (bottom).

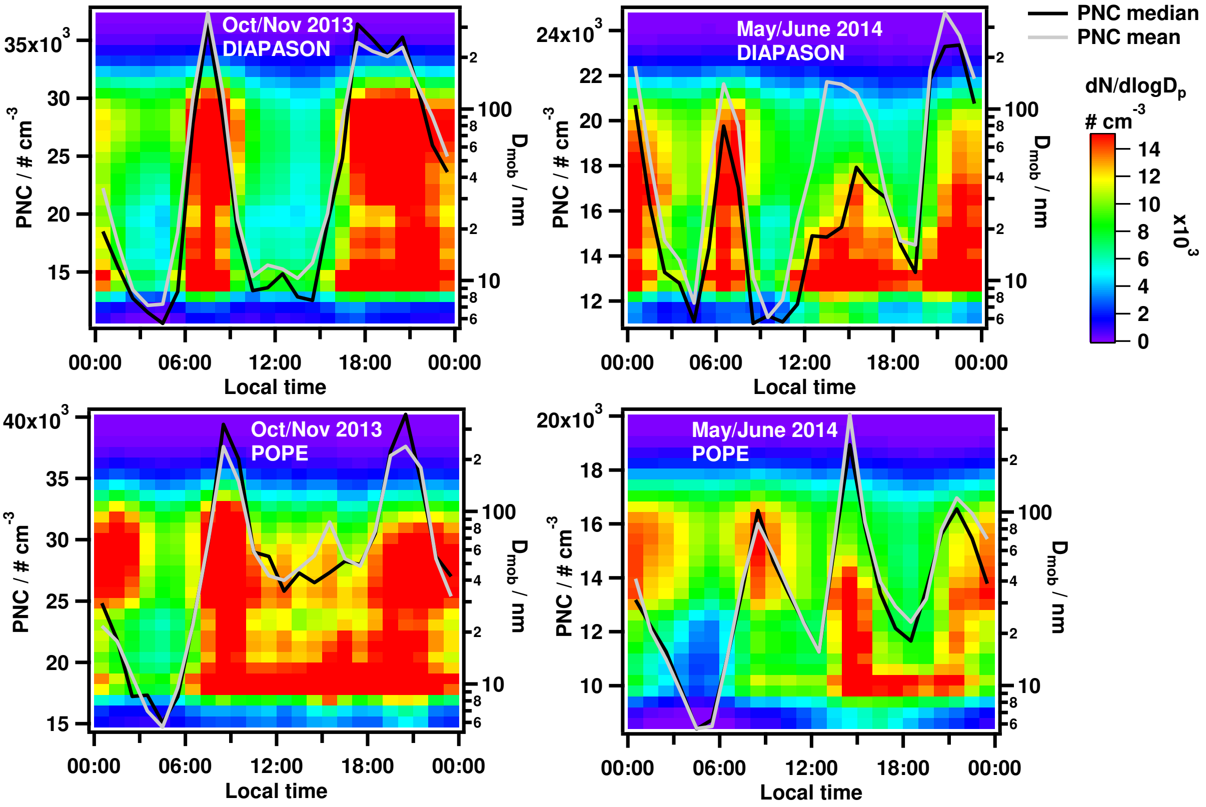

Figure 5. Average diurnal cycles of particle number concentrations and size distributions for DIAPASON (top) and POPE (bottom) for each year (left: 2013, right: 2014). Image plots of diurnal cycles of the particle number size distributions (colour coded for dN/dlogD$_p$) are shown with the particle diameters on the right axes (mobility particle diameter D$_{mob}$). Mean (grey) and median (black) diurnal cycles of the total particle number concentrations are shown on the left axes. New particle formation at midday was only observed in the May/June 2014 campaigns.

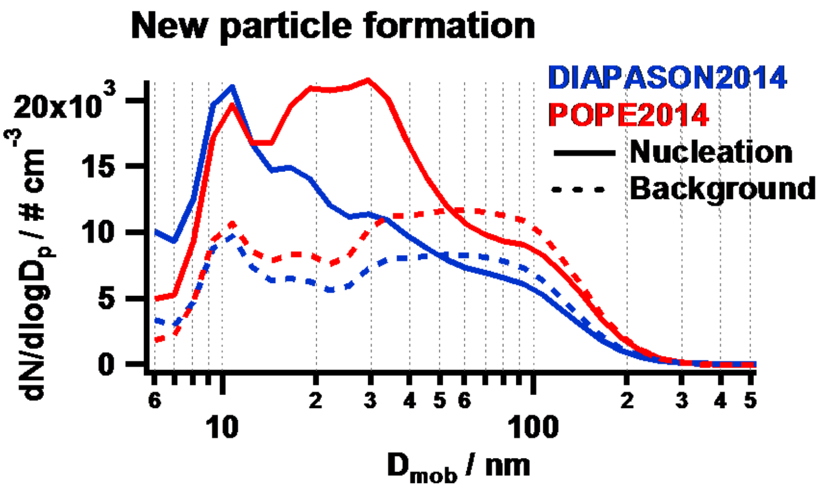

Figure 6. Average size distributions of particle number concentrations (dN/dlogD$_p$) for maximum PNC at midday (DIAPASON2014: 1-3 pm; POPE2014: 2-3 pm; solid traces) and during background conditions (10-11 am; dashed traces) from FMPS measurements for DIAPASON2014 (blue) and POPE2014 (red). D$_{mob}$ is the mobility diameter.

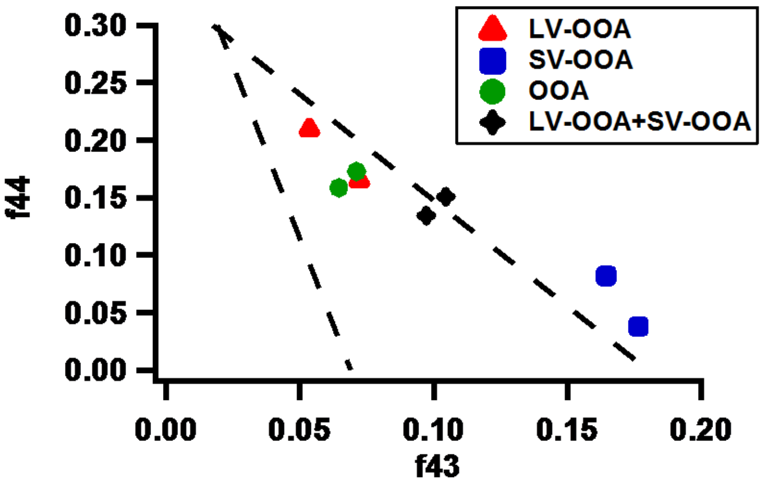

Figure 7. f44 vs. f43 plotted for each OOA factor obtained from PMF analysis of the organic fraction of HR-AMS data. OOA factors (green markers) resulted from DIAPASON2013 and POPE2013 measurements; SV-OOA (blue markers) and LV-OOA factors (red markers) were found during DIAPASON2014 and POPE2014 measurements. The recombination of the factors LV-OOA and SV-OOA for both DIAPASON2014 and POPE2014 is also shown (black markers). The dashed lines represent the triangular space in which measured ambient OOA components typically cluster according to Ng et al. (2010).

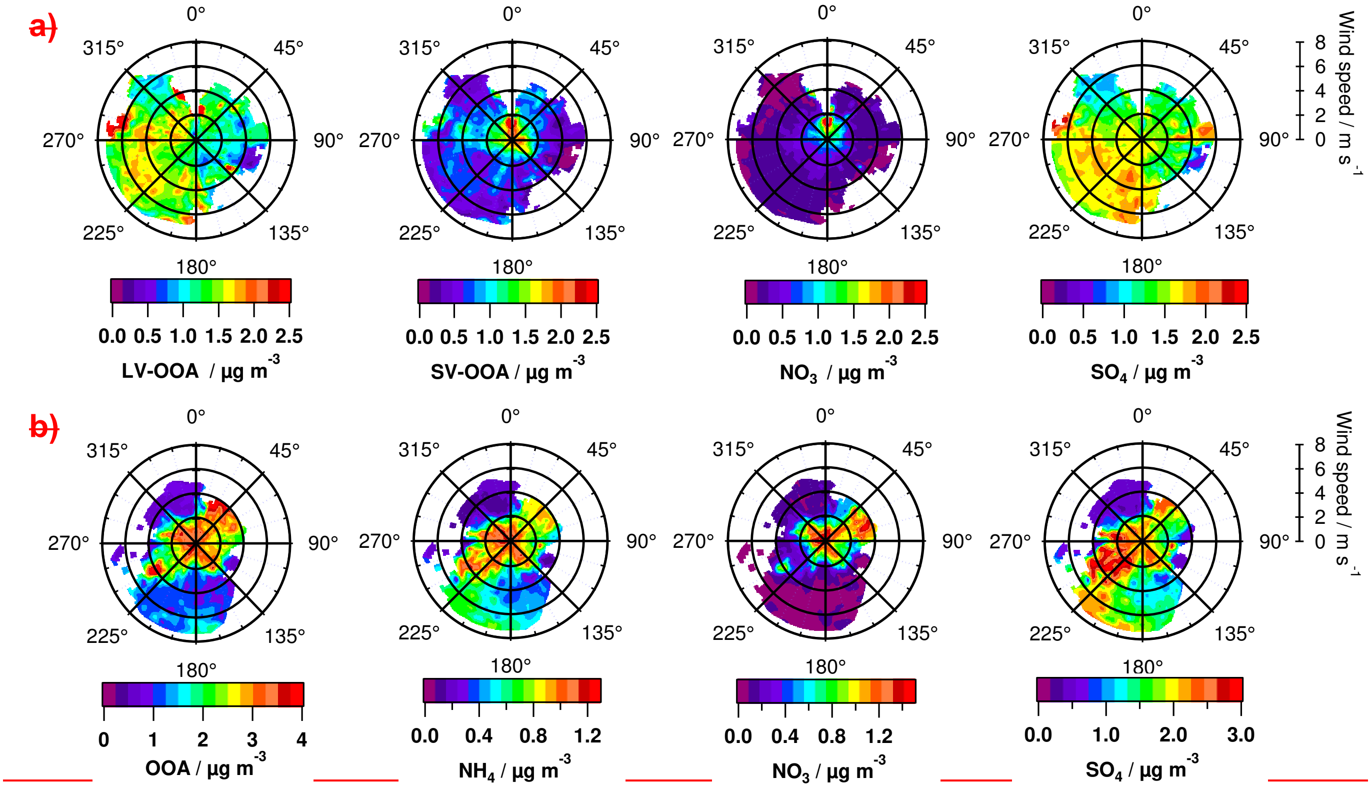

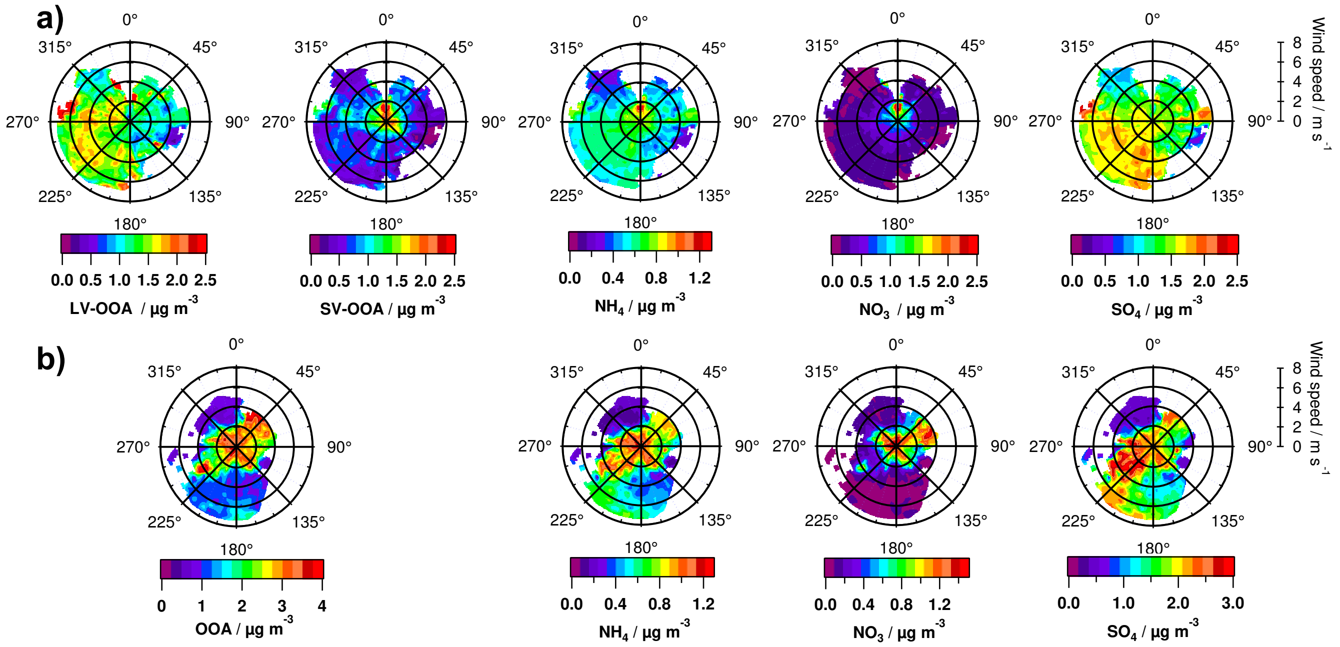

Figure 8. Polar plots of (a) submicron LV-OOA, SV-OOA, NH_4, NO_3 and SO_4 concentration (colour coded) obtained from DIAPASON2014 measurements and (b) submicron OOA, NH_4, NO_3 and SO_4 concentration obtained from DIAPASON2013 measurements as a function of local wind direction (°) and speed (m s^{-1}).

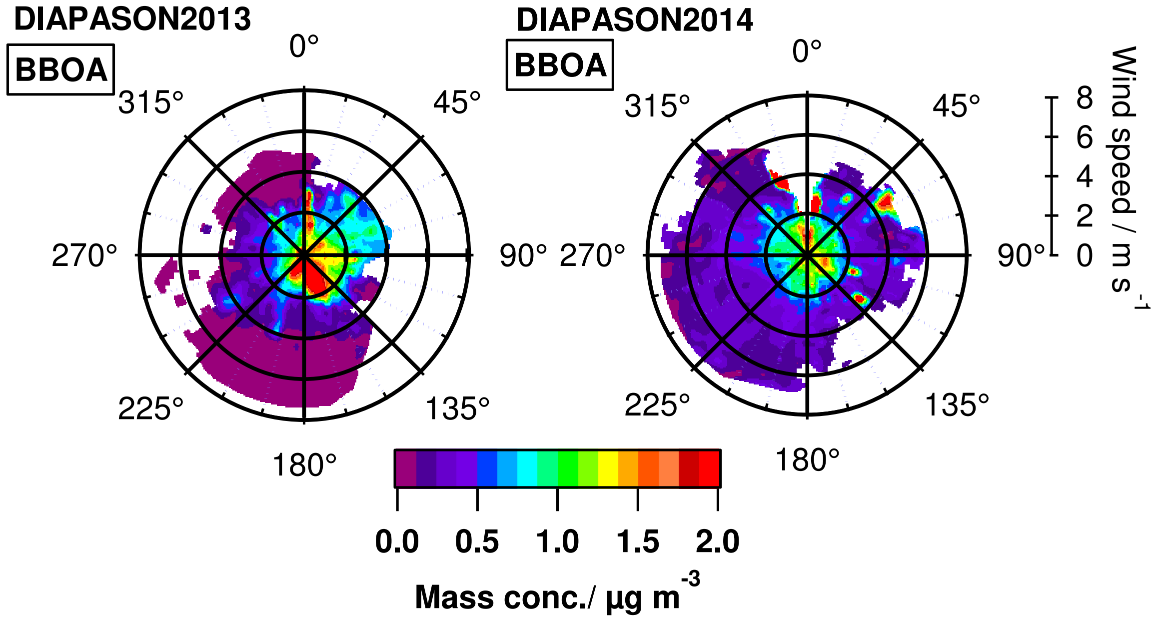

Figure 9. Submicron BBOA mass concentrations (colour coded) as a function of local wind direction (°) and speed (m s^{-1}) for DIAPASON2013 (left) and DIAPASON2014 (right).

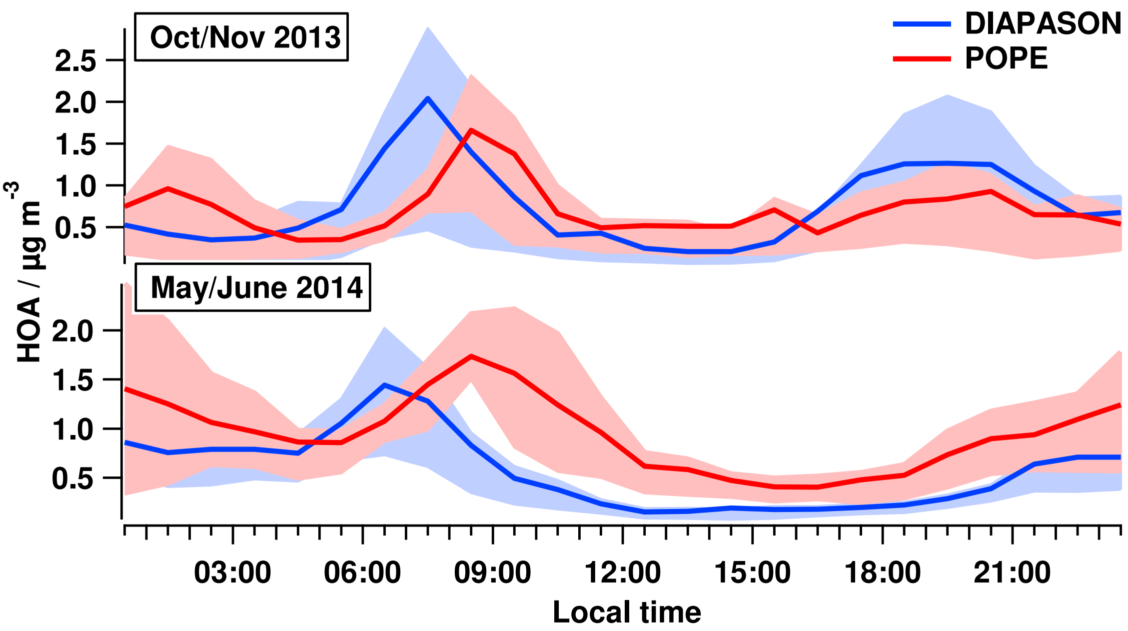

Figure 10. Diurnal cycles of HOA mass concentrations obtained from measurements at Tor Vergata (blue; DIAPASON) and central Rome (red; POPE) during both seasons. Shown are mean concentrations (traces) and the corresponding 25th and 75th percentiles (shaded areas).

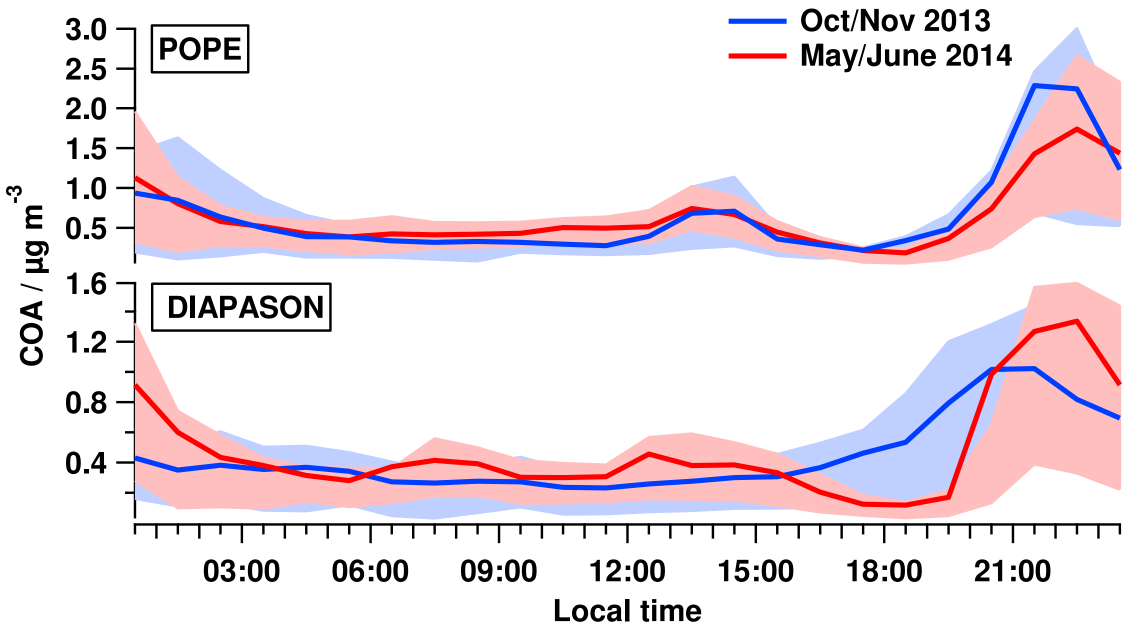

Figure 11. Diurnal cycles of COA mass concentrations observed at central Rome (top; POPE) and the suburban site (bottom; DIAPASON) during both seasons. Shown are mean concentrations (traces) and the corresponding 25th and 75th percentiles (shaded areas).

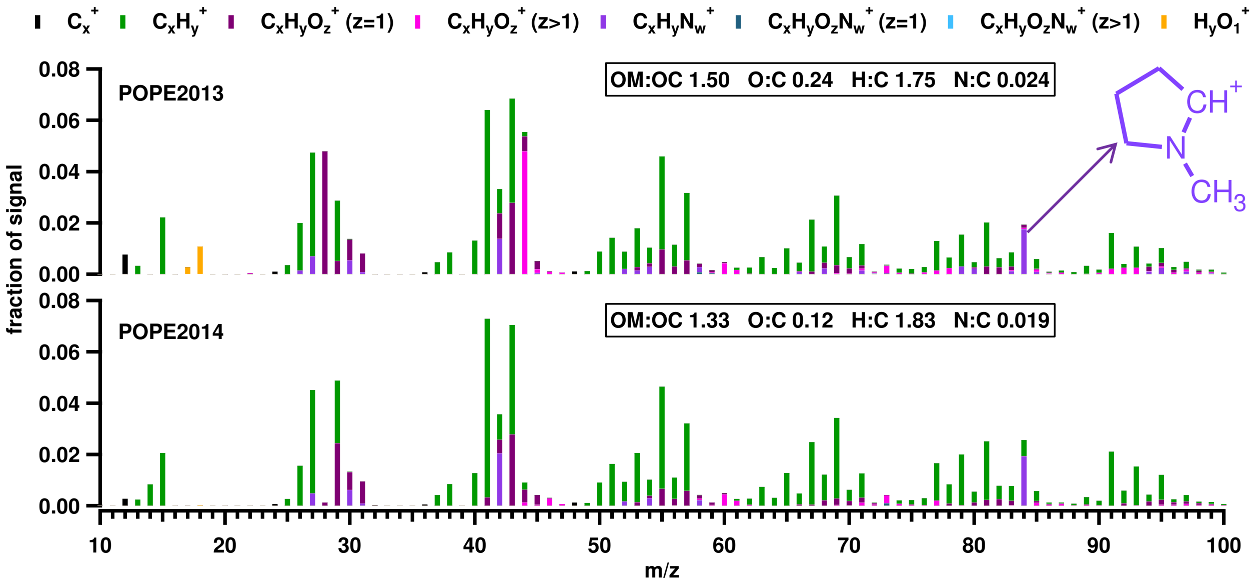

Figure 12. Unit mass resolution spectra of CSOA obtained for the two POPE campaigns, calculated from organic high resolution mass spectra and colour coded for the different groups of ion fragments. The elemental ratios are shown in boxes. The chemical structure of the suggested ion fragment at *m/z* 84 ($C_5H_{10}N^+$) is also illustrated.

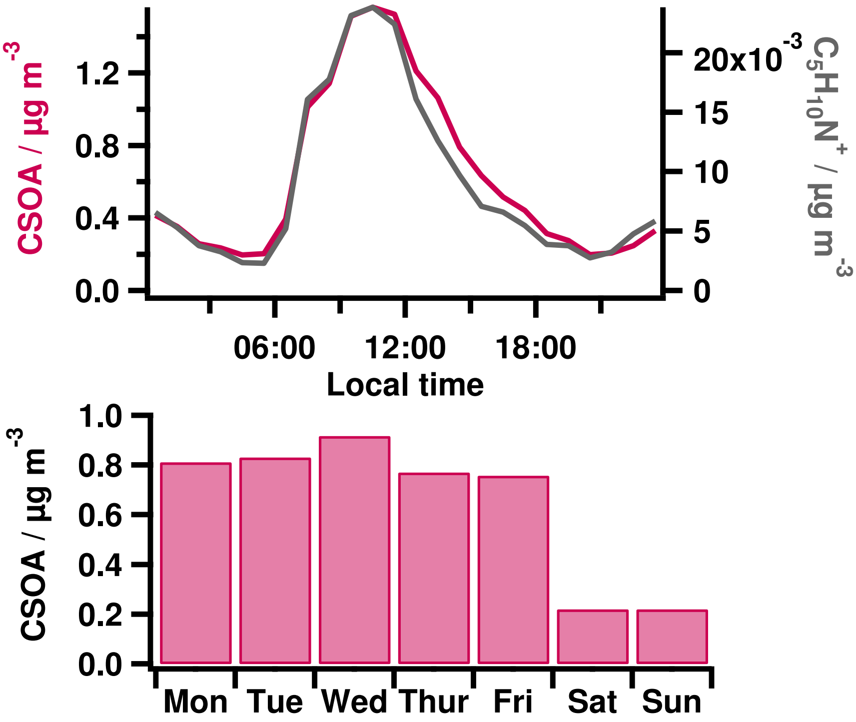

Figure 13. Diurnal cycle of CSOA and the marker fragment $C_5H_{10}N^+$ (top) and the weekly cycle (bottom) of CSOA mass concentrations obtained from HR-AMS data of POPE2014.